Probing Strangeness Production in Proton-Proton Collisions with Three-Particle Correlations

Author
Natalia Melinda Petricean

Supervisor
Alice Ohlson

Fysk03 for 15hp
May 2023
A Bachelor of Science Thesis
Department of Physics, Division of Particle Physics

LUND
UNIVERSITY

Abstract

Strangeness production in small systems such as proton-proton collisions is here investigated through the use of three-particle correlations in the momentum-space coordinates η and ϕ. This method is used in order to investigate possible correlation between conservation of both strangeness and baryon number, such that the particles chosen are $\Lambda\bar{p}K^+$ and the respective charge conjugates, where Λ is a strange baryon, $\bar{p}$ balances: the Balance Function and the comparative restriction of relative positions for pairs of particles within given triplets. The development of normalisation, visualisation and triggering methods are tailored to the problem. The data used is produced by two implementations of the Lund String Model within the Monte Carlo event generator PYTHIA8. Such implementations are the default LSM as well as the string junctions method. The results show a tendency for balancing baryon number and strangeness to be localised nearby, most often close to the strange baryon as well, both in azimuthal angle and pseudorapidity. This signal is less localised within the junction model, which is believed to be more representative of the future phenomenological studies it is intended to compare this research to.

Popular Summary

Particle Physics studies the physics at very small scales. Everything we know is composed of atoms. The atoms then are formed by electrons, neutrons and protons. Electrons are one of the particles that can not be split into smaller components, and therefore it is part of the group of fundamental particles. Neutrons and protons can be split into two types of quarks: up and down. These in turn can not be further split. In total, there exist 6 known quarks. All these elemental particles and their interactions are described by the Standard Model. The Standard Model is so far an extremely successful theory that describes the visible universe. It has been able to predict many of the known particles before they were discovered.

During the first 0.00001 seconds of our Universe's life (to put this into scale, the Universe has existed for 13.7 billion years), the Universe was filled with a hot soup of quarks, anti-quarks and gluons. This hot soup is known as Quark Gluon Plasma or QGP. It is believed that with an understanding of QGP will come an understanding of nuclear matter in the deconfinment regime. This is a very fundamental question and our hopes are high. However, to be able to understand QGP, we would need to study it closely. Is it even possible to do so? QGP seems to have been successfully produced in particle accelerators. However, we are still a long way from understanding how it behaves.

Certain behaviours that we thought indicate the production of QGP and that should only be possible when colliding two heavy nuclei, have also been observed when colliding protons. This doesn't necessarily imply that we were wrong. Rather, it means that we need to take a step back and try to better understand the behaviour and interaction of quarks.

There are heavier quarks than the up and the down. One of these quarks, the strange quark, together with up and down, form particles that are often observed in collisions. Building spatial correlations of where these particles are produced, and what influences said production, will provide some much needed insight into the underlying physics.

A novel way to look at this question is to study such behaviour through the conservation of two quantum numbers: strangeness and baryon number, where strangeness is -1 for every strange quark and +1 for every anti-strange quark, and baryon number is +1 for each particle composed of 3 quarks, and -1 for each particle composed of 3 anti-quarks. This requires the correlation to be done among three particles, where the relative positions of two of them hopefully would result in a tendency for the third one to be localised at certain positions. This would mean that the production of these groups of particles isn't arbitrary and therefore there are some underlying mechanisms to be further studied and understood.

Acknowledgements

First and foremost, thank you Alice, for coming up with such an appealing, engaging and fascinating topic; for believing in me, for patiently listening to my long rambles and picking out the good ideas from there. You turned something as scary as working on a thesis and turned it into a beautiful journey.

Big thanks to Peter Christiansen and Christian Bierlich for clearing out my never-ending questions about Pythia and the Lund String Model. I really enjoyed our conversations. Also, thank you Florido, I would not have gotten ROOT to work without your help.

Also, needless to say I would not have made it this far without Jakob, Jordis, Kim, Noah, Paul and Sora. You guys re-taught me how to enjoy studying and kept me on track throughout the past two years, but more importantly, you've supported me and made me grow as a person. Special thanks to Kim for the enlightening Venn diagrams.

Lastly, I'd like to thank my family. My mom, for teaching me to never stop asking why, to never settle for uncomplete understanding. My dad, for pushing me to reach beyond my limits and pursue physics. My grandma, aunt and uncle for supporting me over the past years.

Contents

List of Acronyms

ALICE: A Large Ion Collider Experiment
CERN: *Conseil Européen pour la Recherche Nucléaire*, European Council for Nuclear Research
OBOS: Opposite Baryon Opposite Strange
SBOS: Same Baryon Opposite Strange
OBSS: Opposite Baryon Same Strange
SBSS: Same Baryon Same Strange
PDG: Particle Data Group
QGP: Quark Gluon Plasma
QCD: Quantum Chromo-Dynamics
SM: Standard Model
ITS: Inner Tracking System
LSM: Lund String Model
TOF: Time Of Flight
TPC: Time Projection Chamber

1 Introduction

With recent observations at the LHC (Large Hadron Collider), where energies are high enough to produce high multiplicity proton proton collisions, as well as heavy ion collisions, a need for subsequent understanding of QCD (Quantum Chromodynamics) has arisen. Questions about Quark Gluon Plasma, an ideal liquid that is thought to have dominated the early Universe, can now be researched through the aforementioned collisions. Nevertheless, the latest observations call for a step back to the basics of the strong interaction. An understanding of simple interactions within small systems and how the quantum numbers are conserved and correlated, if at all, would build a solid foundation for more intricate research.

The aim of this project is to study strangeness behaviour in relation to baryon number conservation within proton proton collisions through a set of simulated data, where strangeness and baryon number are quantum numbers. In order to achieve this, one must correlate a strange baryon with a balancing anti-baryon and a balancing anti-strange particle. For this purpose, three-particle correlations are hereby used, a novel method that has not been explored in detail to the date of this research.

Such three-particle correlations are constructed with respect to the spatial coordinates ϕ and η, between particles 1, 2 and 1, 3, such that they yield 4 dimensional histograms. As the strange baryon, particle 1 is taken to be $\Lambda(\bar{\Lambda})$, being the trigger particle, and particles 2 and 3 are $\bar{p}(p)$ and $K^+(K^-)$ respectively as balancing anti-baryon and balancing anti-strange meson. The difficulty of visualising a 4D histogram arises, which is another goal item for this research, for which projection methods are used.

To develop an understanding of these three-particle correlations, two approaches are taken. On one hand, the Balance Function is built to select the pure three-particle correlations, removing apparent correlations where only two or no particles are produced within the same interaction. On the other hand, ranges within the correlations of two of the particles are set, allowing us to explore what that implies for the third particle.

The data used for the development of the three-particle correlations was simulated through PYTHIA8, a Monte Carlo based event simulator, which allows for different hadronisation models to be selected. The long term scope of this research is for future data yielded by the ALICE detector at CERN [1] to be contrasted with the hereby presented results.

2 Theory

2.1 Standard Model and Quantum Chromo-Dynamics

The Standard Model is a theory that successfully describes the fundamental particles that all known matter is made of and three of the fundamental forces of nature: the Electromagnetic, Weak and Strong Force. The particles shown in table 1 are split into two main categories: fermions and bosons. Fermions are particles with half-integer spin while bosons have integer spin. All force carriers are bosons, while the fermions split into quarks and leptons. Quarks are the particles that interact through gluons, which

are gauge bosons and the force carriers of the strong force. This force is described by the gauge theory of quantum chromodynamics, QCD for short. The naming derives from the distinction between this group of particles and the rest through the presence of the colour quantum number. [2]

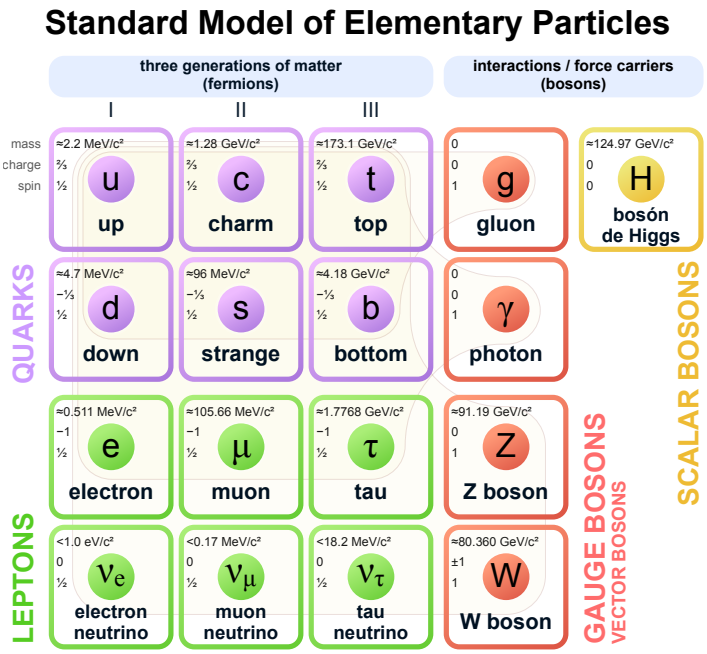

Figure 1: Standard Model of Elementary Particles. Figure taken from Wikimedia Commons [3]

The colour quantum number has six possible values: green, red, blue and anti-green, anti-red and anti-blue. Colour charge changes under charge conjugations such that the charge conjugate of red r is anti-red $\bar{r}$, g to $\bar{g}$ and b to $\bar{b}$. Quarks also have electric charge and they are divided into two groups: up, down and top have a charge of 2/3 while down, strange and bottom have a charge of -1/3. One feature of QCD is colour confinment. This implies that particles that are not colour-neutral cannot be isolated. While quarks only have one colour value, gluons have two. The five possible colour-neutral combinations for hadrons (particles composed of quarks) are seen in Figure 2. Gluons interact with all coloured particles, which gives

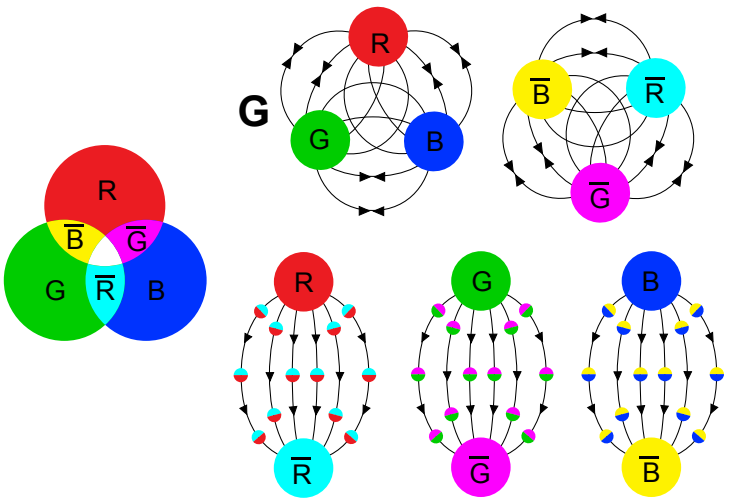

Figure 2: colour quantum number and the five neutral colour combinations of hadrons. Figure taken from Wikimedia Commons [4]

QCD the special feature of a gauge boson that interacts with itself as well as with the corresponding fermions.[5]

Quarks arrange themselves into hadrons such that they are colour neutral, the two main categories of which are baryons composed of three quarks or three anti-quarks, qqq or $\bar{q}\bar{q}\bar{q}$ and mesons, with a $q\bar{q}$ pair [2]. The strong force gets its name from the strong coupling constant. This coupling constant, among other things, dictates how much energy needs to be put into a system of $q\bar{q}$ to decouple it. Up until a limiting point, the further apart two quarks are pulled, the stronger the field becomes and the more energy needs to be put into the system. Eventually that energy will result in a new $q'\bar{q}'$ pair such that two new pairs of $q'\bar{q}$ and $q\bar{q}'$ are formed. This process can be repeated several times inside a particle collider, which results in jets. Simultaneously, at distances smaller than 1 fm (which is about the size of a hadron) asymptotic freedom is found, such that quarks move freely within hadrons. Moreover, this property is also found at increasing energies and temperatures. [2] [5]

Within strong interactions overall, there are certain conserved quantities like baryon number and quark flavor. The starting particles and end products within a collision will conserve total baryon number and total flavor quantum number, such that if initially there are no baryons, the total baryon number of the final products should also be zero. This can be achieved with, for example, a baryon and an anti-baryon. The same is applicable to quark flavors; up, down, charm, strange, top and bottom.

While strangeness conservation is property of QCD, it is not necessarily conserved in the Weak interaction due to Flavor Changing Charged Currents. However, the probability of these interactions happening is the same for all triplets of particles, and thus this is later accounted for implicitly, see section 3.1.

2.2 Quark Gluon Plasma

The Quark Gluon Plasma (QGP) is thought to be formed in heavy ion collisions [6] [7] in the form of small droplets. This liquid is composed of partons (gluons and quarks) and a characteristically small viscosity, such that it is near the quantum lower bound [8]. During heavy ion collisions, partons described by perturbative QCD are formed, as well as quarks and gluons described by non-perturbative QCD. These partons will form QGP throughout their thermalisation, which results in a process known as hydrodynamic flow. High pressure gradients drive the expansion of the system relative to the plane of symmetry, producing anisotropic flow. This implies that the QGP is composed of strongly coupled matter with a small mean free path. The anisotropic nature of the interaction region is present both in position and momentum space. Another signature of quark gluon plasma produced in heavy ion collisions is jet quenching. This occurs when the high energy particles interact with the medium, thus reducing their energy drastically [9], which makes the produced jets to have a broader and softer appearance.

Previous work has measured two-particle correlations in proton-proton collisions as well as in proton-heavy ion and heavy ion - heavy ion collisions. This has yielded comparative results in terms of distribution of produced particles in momentum-space coordinates.

Some of the flow signatures previously attributed to QGP have been unexpectedly observed in smaller systems. Some of these flow effects are hard to distinguish from the commonly occurring jets within such small systems [10] [11].

The research question asked in this thesis project stems from the latter problem: is it possible to distinguish collective behaviour from the rest of phenomena? Can this be done through three-particle correlations?

2.3 Coordinate System

The coordinate system used in this research is composed of the pseudorapidity η and azimuthal angle ϕ. Pseudorapidity is defined in terms of the longitudinal angle θ between the three momentum p and the positive beam axis:

$$\eta \equiv -\ln\left(\tan\left(\frac{\theta}{2}\right)\right). \tag{1}$$

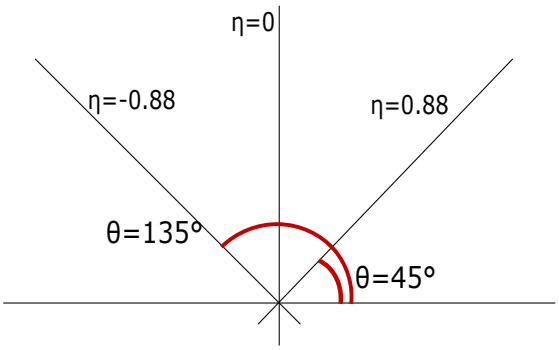

Figure 3: Visualization of η from $\theta = 45°$ to $\theta = 135°$

An angle $\theta = 45°$ yields $\eta \approx 0.9$. For the purpose of this thesis work, the particles are analysed in the pseudorapidity range of $|\eta| < 1$ given that the aim is to eventually reproduce the results found here with data from the ALICE detector at CERN [1], which has an Inner Tracking System acceptance of $\eta = 0.9$.

At mid-rapidity, the ALICE detector has full 2π acceptance in the azimuthal angle ϕ, the angle in the plane perpendicular to the beamline.

In figure 4, 3 different values of η are collected together with a range around 0 in ϕ. The longer the green inverted cone, the larger the η value. An η value of 0 is thus perpendicular to the beam line.

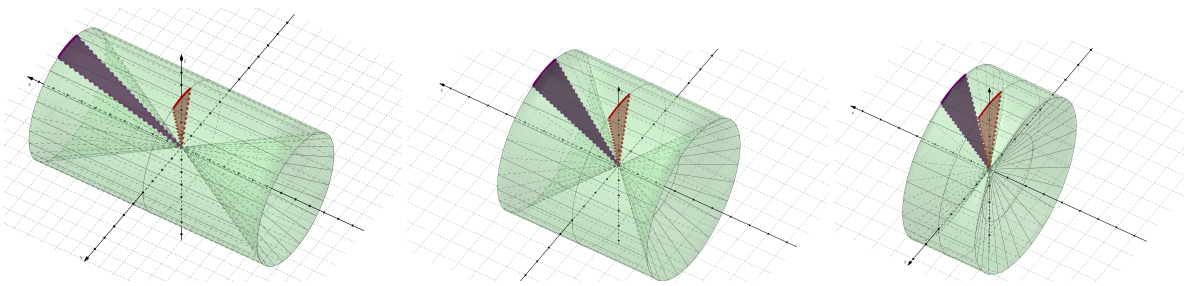

Figure 4: Vizualization of η against ϕ, where the green are represents η, the red are represents ϕ, and the purple area´is the intersection. From left to right, decreasing η.

2.4 Particle Correlations

Two-particle correlations in terms of spatial angular coordinates have been mostly used for the purpose of illustrating how two particles are situated with respect to each other. This results in histograms that correlate pairs of particles within events, showing a correlated behaviour of particles across collisions. With this purpose in mind, the η, ϕ coordinates are used [12].

Three particle correlations have not been explored in depth. The principle is the same, with the added benefit that one can observe the correlated behaviour of three particles instead of two. The normalisation methods used in this thesis rely on the amount of triggers across events. For the purposes of this thesis, the triggers used are the total number of $\Lambda(\bar{\Lambda})$ baryons that have been produced through PYTHIA8, as well as alternative counting of triggers for the projections of the three-particle correlations within given ranges, explained below.

2.4.1 Balance Function

In order to correct for the range limit of the η coordinate, a correlation is built with particles from separate events such that they are in fact completely uncorrelated. The result is used to correct the shape of the distribution of correlated particles through a division of histograms. This is done by normalising the uncorrelated events to a maximum of 1. Once this is done, the two normalisation methods explained below are applied to the corresponding correlations.

In all cases, the 4 dimensional correlations are normalised by the number of triggers, as well as the width of the bins for $\Delta\eta_{12}, \Delta\eta_{13}, \Delta\phi_{12}, \Delta\phi_{13}$, which are the resulting correlations between particles 1, 2 and 1, 3. It follows from:

$$C(\Delta\eta_{12}, \Delta\eta_{13}, \Delta\phi_{12}, \Delta\phi_{13}) = \frac{1}{N_{trig}} \frac{d^4N}{d\Delta\eta_{12}d\Delta\eta_{13}d\Delta\phi_{12}d\Delta\phi_{13}}, \tag{2}$$

where the value yielded by C corresponds to the number of associated particles at a given $\Delta\eta, \Delta\phi$ from the trigger Λ.

When, for visualization purposes, projections are done of these 4 dimensional histograms, an adjustment of the equation 2 is done. Mathematically, a projection of such histograms requires an integration over the variables that one projects against. If the projection will show $\Delta\eta_{12}, \Delta\phi_{12}$ it means that one is integrating over $\Delta\eta_{13}, \Delta\phi_{13}$, such that the following expression is used:

$$C(\Delta\eta_{12}, \Delta\eta_{13}, \Delta\phi_{12}, \Delta\phi_{13}) = \frac{1}{N_{trig}} \int_{\Delta\phi_{12}} \int_{\Delta\eta_{12}} \frac{d^4N}{d\Delta\eta_{12}d\Delta\eta_{13}d\Delta\phi_{12}d\Delta\phi_{13}} d\Delta\eta_{12}d\Delta\phi_{12}. \tag{3}$$

2.4.2 Ranges

An alternative method to analyse three-particle correlations is formulated. Within the correlations stored in THnF (a n-dimensional ROOT histogram), one can select particles

1 and 2, in this case the two baryons, to be constrained in $\Delta\phi$ and/or $\Delta\eta$. Consecutively, one can observe which are the tendencies, if any, of the third particle. In order to check whether such tendency is caused by the restriction and is not simply a general behaviour that can be observed at any selected range in $\Delta\eta$ or $\Delta\phi$, a division between the restricted histogram and the non-restricted histogram is made.

Conducting such a procedure yields a mathematical expression which is that of an integral over a restricted integration range of the selected variables. If one aims to evaluate the function at a given range R_η for $\Delta\eta_{12}$ and R_ϕ for $\Delta\phi_{12}$, the expression becomes:

$$C(\Delta\eta_{12}, \Delta\phi_{12}) = \left(\frac{1}{N_{trig}} \frac{d^4N}{d\Delta\eta_{12} d\Delta\eta_{13} d\Delta\phi_{12} d\Delta\phi_{13}} \right)_{d\Delta\eta_{12}\in R_\eta,\ d\Delta\phi_{12}\in R_\phi}, \tag{4}$$

which yields a need for a different triggering method. This triggering method is found through the counting of all the particle pairs 1 and 2 within the given ranges R_η, R_ϕ.

2.5 Detection of Particles

The particles that one would be interested in detecting in order to be able to reproduce the results within this research are $\Lambda, \bar{\Lambda}, K^+, K^-, p, \bar{p}$. Charged kaons and protons are long lived, and thus can be detected through direct tracking. On the other hand, $\Lambda, \bar{\Lambda}$ must be detected through their decay products. The most common decay products that can be used to detect them at the ALICE detector are protons and charged pions, with a branching ratio of 63.9% [13].

$K^+, K^-, p, \bar{p}$ are detected with the Time Projection Chamber or TPC [1]. They can be distinguished through a plot of their energy loss per unit distance, fitted with a Bethe-Bloch curve. Where these energy deposition curves overlap, the time of flight TOF method is used such that with the velocity and momentum inputs one can solve for mass. These processes are illustrated in figure 5.

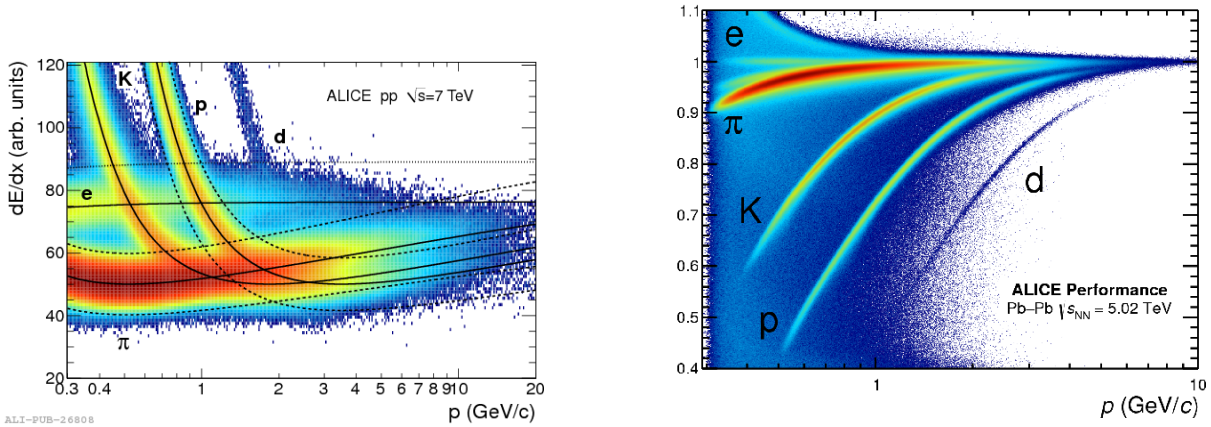

Figure 5: (Left) Energy deposition as a function of momentum from TPC, taken from [14]. (Right) TOF method for particle identification, taken from [15].

The detection of the strange baryon is done through identification of the $p\pi^-(\bar{p}\pi^+)$ pair with the aforementioned methods, and track reconstruction, such that both should meet

at an interaction point displaced from the primary vertex. The counts of $\Lambda(\bar{\Lambda})$ found through this process are divided by the branching ratio of such process, thus inferring the total number of Λs.

2.6 Pythia: inner workings

Particle production within PYTHIA8, a Monte Carlo particle generator [16], can be achieved through the use of different mechanisms. These mechanisms follow theoretical predictions that describe how particle generation processes occur. Within this project, two such mechanisms are explored within the Lund String Model: the baseline model and with junctions turned on, both of which describe hadronisation processes.

2.6.1 Lund String Model

The Lund String Model treats partons as coloured field lines that collimate due to the self-interacting nature of gluons. In the simplest cases, these strings connect a $q\bar{q}$ pair, and hadrons are produced when such strings are fragmented, producing 1 or 2 new pairs of quarks at each fragmentation point. This process requires that adjacent baryons share 2/3 of their colour quantum numbers, as seen in figure 6, and thus results in restrictive production conditions.

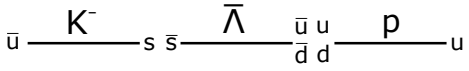

Figure 6: Simplified example of a string breaking.

These strings are oriented along the beamline. In the case of $\Lambda, K^+, \bar{p}$, this process will more often produce the Λ baryon in between the proton and kaon. The quarks produced at string breaking points are required to have compensating transverse momenta such that their addition in the string's momentum frame yields zero. The sum of the p_T of the ends of the broken string pieces will yield the momentum of the hadron. If the string is produced through hard scattering, this implies the Λ will be located back to back with respect to both the kaon and proton, observed in ϕ, whereas they would all share similar pseudorapidity which can be qualitatively understood by the fact that the momenta of strange quarks is comparable to the momenta of an up-down di-quark given their approximate masses, while the Λ being a heavier baryon will take most of the momentum fraction, as two balancing effects. However it is likely for the Λ baryon to have a momentum independent of the $K^+, \bar{p}$, while the similarity in p_T for the kaon and proton is still held. [17]

Another possible picture known as the popcorn mechanism, which has been observed experimentally [18], is the breaking of a colour string to produce a "meson in-between". In figure 7 a sequence of steps is shown, in which first there exists a colour string from red to anti-red, in which a green anti-green fluctuation is observed. This fluctuation generates a string equivalent to an anti-blue to blue string, on top

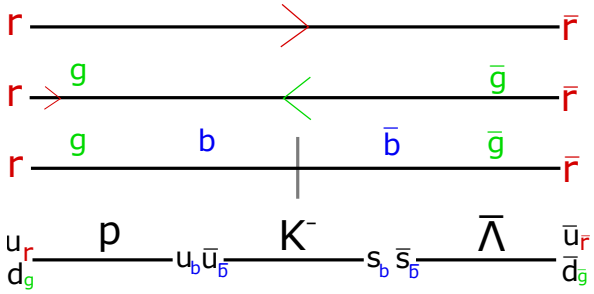

Figure 7: Example of the popcorn model.

of which a second fluctuation of blue to anti-blue may occur, yielding a colour neutral string which can now break into two baryons. The experimental results have shown, however, that on average around 1 meson is produced between these two baryons, a value which is highly dependant on the kinematics. In PYTHIA8 this is set to a constant of 1 [17]. Such a situation would yield a $\bar{\Lambda}$-K^--p ordering close both in ϕ and η.

2.6.2 Junctions

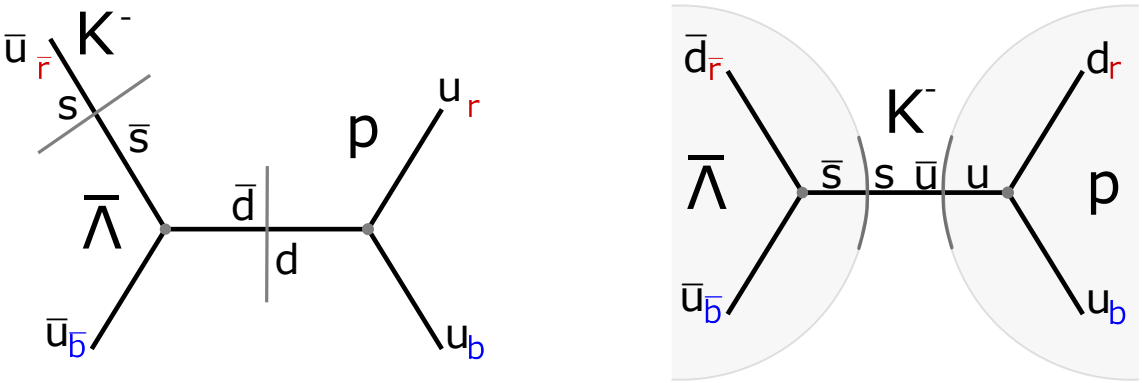

Figure 8: (Left) Example of junctions method without correlation across the three particles. (Right) Example of junctions method with all 3 particles correlated.

Junctions take a step further within the string model with the added feature that two strings can merge into one, the intersection point of which is the junction, that must now be balanced, usually by an anti-junction, such that the two end-points are respectively the opposite colours of the two start points. As shown in figure 8 (left), if a $q\bar{q}$ tunnels out of the vacuum, breaking the merged section of the string, two baryons are produced. In order for one of them to be a Λ baryon, there needs to be a s-quark at one of its 3 end-points.

While it is likely that this string breaking would occur on one of the legs, and not between the junctions, this would yield a meson completely uncorrelated to the proton in the udu-junction (up-down-up), as seen in figure 8 (left).

Therefore, the only correlated possibility would be for the meson to appear in between junctions, such that there are two breaking points, as shown in figure 8 (right). In this case, the kaon and the proton would be found closer to each other than to the Λ, similarly as in the default case, since the strange string breaking takes most of the momentum fraction, yielding the remaining hadrons closer in η.

3 Method

3.1 Observables

3.1.1 Balance Function

One of the aims of this project is to define and illustrate the Balance Function for three-particle correlations, composed of the $\Lambda, \bar{\Lambda}, p, \bar{p}, K^+, K^-$ hadrons. The Balance Function

should represent the pure correlation between $\Lambda, K^+, \bar{p}$ (and similarly for the equivalent charge conjugates $\bar{\Lambda}, K^-, p$). This is the single combination that balances baryon number and strangeness. In order to achieve the correlation where all three particles are correlated directly, one has to compensate for random triplets that are not completely correlated but still show up in the initial three particle correlation. The probability for those random triplets to occur should be comparable to the amount of random triplets of other combinations, i.e. the 3-particle correlations for triplets occurring from different processes or string breakings within the same event. By random triplets, or uncorrelated triplets, one means triplets within which one or more of the particles are produced independently of the others.

There exist 6 such triplets. Firstly, where the Λ, K^+ two-particle correlation is combined not with an antiproton, but a proton such that the triplet Λ, K^+, p is formed, as well as the charge conjugate $\bar{\Lambda}, K^-, \bar{p}$. Here there is the balancing strangeness, whereas the balancing anti-baryon is missing. This mimics the chance of the balancing anti-baryon not being a result of the same string as the strange hadrons, and should therefore account for such randomness. Secondly, the case in which the uncorrelated particle is the kaon, such that the triplet $\Lambda, K^-, \bar{p}$ is formed, as well as the charge conjugate $\bar{\Lambda}, K^+, p$. Here one can see the case where the same strangeness is known to be uncorrelated and is expected to mimic the cases where the balancing strangeness happens to be uncorrelated. This however removes once too many times the completely random triplets, since both these cases include the possibility for all three particles to be uncorrelated. Thus, the three particle correlation for $\bar{\Lambda}, K^+, \bar{p}$ and the charge conjugate Λ, K^-, p is added back once, yielding the Balance Function, i.e. Balance Function = [Opposite Baryon / Opposite Strange] - [Same Baryon / Opposite Strange] - [Opposite Baryon / Same Strange] + [Same Baryon / Same Strange] = OBOS - SBOS - OBSS + SBSS. The Balance Function is visualised in figure 9. This Balance Function already takes care of the less dominant effect of flavor changing weak interactions, since the same probability is added and subtracted twice and eventually cancelled out, which is relevant when testing it on data collected experimentally. However, for the purpose of this thesis, weak decays are turned off. See section 3.2.

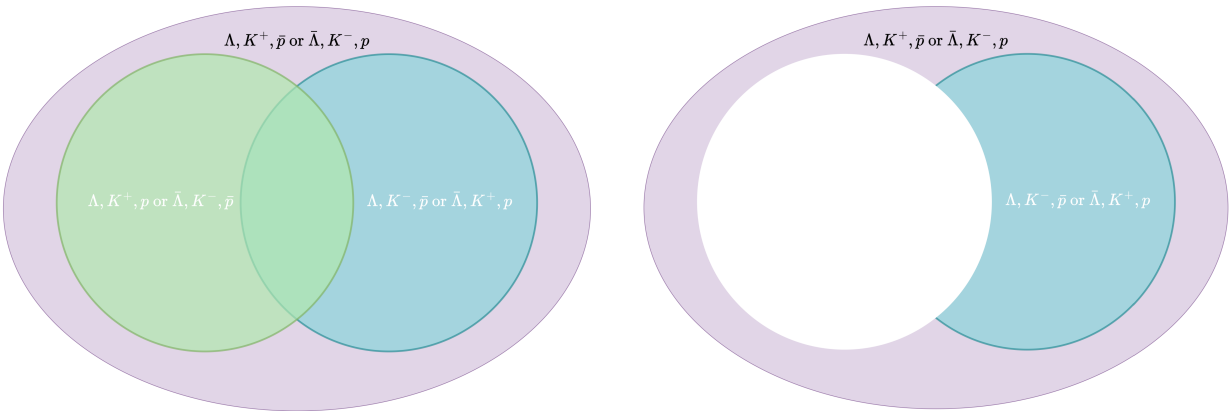

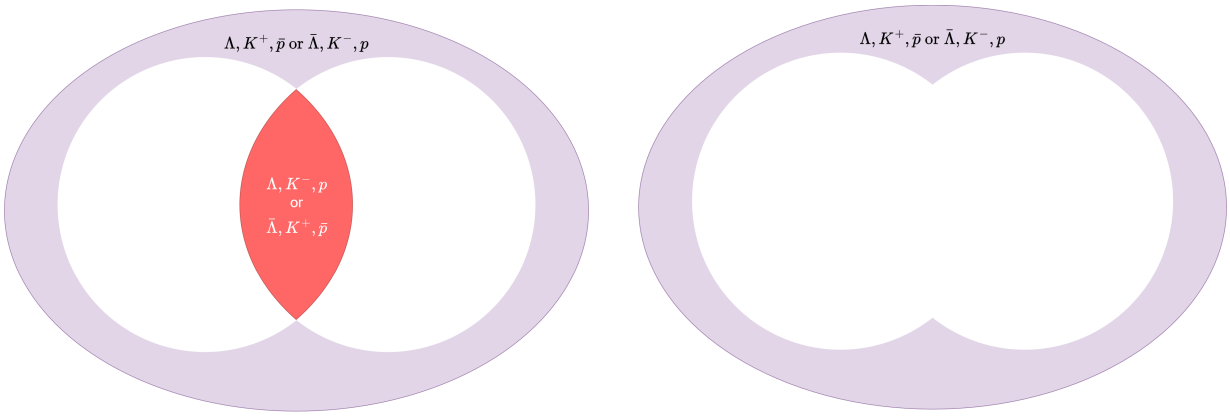

Figure 9: Venn diagram schematic of the Balance Function steps.

3.1.2 Ranges

In order to define the observable for the visualization described in section 2.4.2, ranges are set in $\Delta\eta$ and $\Delta\phi$ taken between the $\Lambda, \bar{\Lambda}$ and $p, \bar{p}$. The chosen ranges are of $|\Delta\eta_{12}| < 0.2$ or no restriction, and $|\Delta\phi_{12}| < 0.3$ or $|\Delta\phi_{12} - \pi| < 0.3$, thus giving 4 combinations. Then, $\Delta\phi_{\Lambda,K}$ against $\Delta\eta_{\Lambda,K}$ is projected for such a restriction in the protons, for all triplet combinations.

Subsequently, they are normalised in a similar fashion to the Balance Function, except the triggering method is adapted to the visualization purposes of this approach. All appearing pairs of baryons are counted and split in two groups: same baryon number $\Lambda(\bar{\Lambda}), p(\bar{p})$ and opposite baryon number $\Lambda(\bar{\Lambda}), \bar{p}(p)$. These are applied correspondingly to the four triplets' projections in $\Delta\eta_{\Lambda K}, \Delta\phi_{\Lambda K}$ without any range selection for the Λp pair. Consequently, the projections resulting from a range selection are triggered with all appearing pairs of $\Lambda(\bar{\Lambda}), p(\bar{p})$ and $\Lambda(\bar{\Lambda}), \bar{p}(p)$ within the range in question, since one aims to produce the distribution of associated kaons per Λp pair.

Ultimately, these selected pair projections of ΛK are integrated over $\Delta\eta$ and the binwidth is multiplied back in, yielding TH1F histograms (one-dimensional ROOT histograms). The same is done for the non biased correlations. As a last step, all ranges are divided by the corresponding no-range projections, such that the profile of the 1 dimensional plots showcases the qualitative comparison between what is expected and what is actually observed. If there was no difference of $\Delta\eta$ and $\Delta\phi$ choices with respect to the general result, this method would yield a flat histogram at a constant of 1.

3.2 Pythia: Particle Generation

PYTHIA8 was used to generate events and save the triplets of interest in a TTree, a type of data structure used in ROOT. Code written in a C++ file importing PYTHIA8 was set to select events that contained any triplet of interest and save only such events containing said particles. This was done using the PDG (Particle Data Group) codes for Monte Carlo methods [13] with $\Lambda = 3211, \bar{\Lambda} = -3211, p = 2212, \bar{p} = -2212, K^+ = 321, K^- = -321$. All $\Lambda, \bar{\Lambda}$ particles were counted and saved in a histogram, even if said particles were not used for a later correlation as they would count as triggers. Two methods of particle gen-

eration were used: firstly, the standard Lund String Model, and secondly using junctions.

For both methods, four sets of parameters were used for the correlation: the corresponding ϕ and η values of the particles, the total $\Lambda, \bar{\Lambda}$ for triggering and the corresponding PDG values of the particles.

A code snippet for enabling junctions through PYTHIA v8.309 is shown in Appendix B.

3.3 Toy Model and Two Particle Correlation

Before building the three particle correlation that would use the events and particles generated through PYTHIA8, a simple model using ROOT ADDED a citation [19] with C++ was built to test the understanding of two-particle correlations independently of the particles used. For that purpose, a simple pseudo-random number generator was used for η and ϕ values within the ranges $|\eta| < 1$ and $0 \leq \phi \leq 2\pi$. In order to emulate jets, a Gaussian distribution of width $\sigma = 0.1$ with μ being a pseudo-random value within the η or ϕ range. Then, pseudo-random values ϕ_1 and η_1 following said Gaussian distribution were extracted. For the back to back jet, the following relation was made:

$$\phi_2 = \phi_1 + \pi \qquad \text{if } \phi_1 < \pi, \tag{5}$$

$$\phi_2 = \phi_1 - \pi \qquad \text{if } \phi_1 > \pi, \tag{6}$$

while η_2 was kept independent of η_1. For every event, n randomly distributed particles were generated, n particles within one jet and n within the back to back jet.

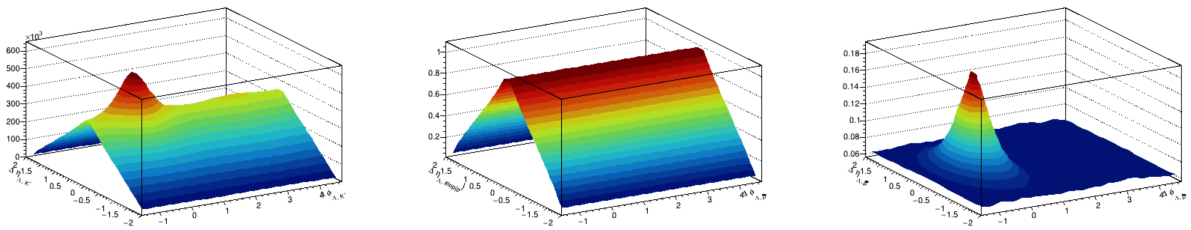

Figure 10: Plot obtained with the toy model. The signal (right) is obtained through dividing the correlations (left) by the normalised acceptance (center).

Next, a simple two particle correlation was built. The particles generated in event m were correlated by finding their difference in η and ϕ, such that $\Delta\eta = \eta_i - \eta_j$ and $\Delta\phi = \phi_i - \phi_j$. These were stored in ROOT histograms. To correct for the detector acceptance, the 10 previous events were saved and a two-particle correlation was built across events such that particle i and particle j belonged to two different events. This $\Delta\phi_M$ and $\Delta\eta_M$ were saved in a mixed events histogram that was consequently normalised to a maximum of 1. Thus, the signal is found when dividing the correlation histogram by the mixed events histogram.

Since the interesting parts of the plot are localised at $\phi = 0, \pi, 2\pi$, the plotting range was set such that $-\pi/3 \leq \Delta\phi \leq 2\pi/3$. If $\Delta\phi$ was out of those bounds, its value was corrected by adding 2π if it was lower or subtracting 2π if it was higher, yielding its equivalent angle.

3.4 Three-Particle Correlation

The TTree generated by the PYTHIA8 file was read and the branches of interest were selected within each event. Consecutively, within each event the particles were sorted in 6 categories according to their PDG codes, later used for the three-particle correlations. The correlations were built for each of the 8 possible triplet combinations, with the η and ϕ values iterated such that $\Delta\eta_{12}, \Delta\phi_{12}$ would refer to the correlation between $\Lambda(\bar{\Lambda}), p(\bar{p})$ and $\Delta\eta_{13}, \Delta\phi_{13}$ between $\Lambda(\bar{\Lambda}), K^{\pm}$, such that the $\Lambda(\bar{\Lambda})$ in question is the same in both correlations. The same correction from the toy model for the $\Delta\phi$ ranges was used.

For the detector acceptance correction, a matrix of 10 past events containing the latest $p, \bar{p}, K^+, K^-$ lists with η and ϕ values was saved. These were accessed and the same 8 correlations were made, where the $\Lambda, \bar{\Lambda}$ within the current event were correlated to the corresponding $p, \bar{p}$ and K^+, K^- from different events.

Each triplet correlation together with its charge conjugate equivalent, both within events or in mixed events, was saved in a THnF of four dimensions, i.e. a four dimensional histogram. For the plotting, for visualization reasons each THnF was projected into four two dimensional histograms: $\Delta\phi_{12}$ against $\Delta\phi_{13}$, $\Delta\eta_{12}$ against $\Delta\eta_{13}$, $\Delta\phi_{12}$ against $\Delta\eta_{12}$ and $\Delta\phi_{13}$ against $\Delta\eta_{13}$. All operations done on the histograms were done on their projections since they are not defined for THnF histograms. Those operations entail: first, the normalisation to 1 of the acceptances; secondly, the histograms of correlations within events were divided by the corresponding normalised acceptances, thus removing affects of the detector acceptance. The resulting histograms were normalised by dividing by the bin widths of the projected axes and by the total triggers corresponding to the given method, thus yielding the effective signals.

4 Results and Discussion

The plots presented in this section are the ones considered relevant for discussion. To look at all the plots produced for this research, see Appendix A.

4.1 Three particle correlations: $\Delta\phi_{12}$ vs. $\Delta\phi_{13}$

4.1.1 Default Lund String Model (LSM)

In figure 11, the three-particle correlations projected on $\Delta\phi_{12}$ and $\Delta\phi_{13}$ are displayed for all possible triplets such that the charge conjugates of each triplet are contained within the same plot. This was done given that plotting the charge conjugate correlations independently of each other did not contribute with any new information. This does not necessarily have to be the case if this analysis is done on data collected at CERN.

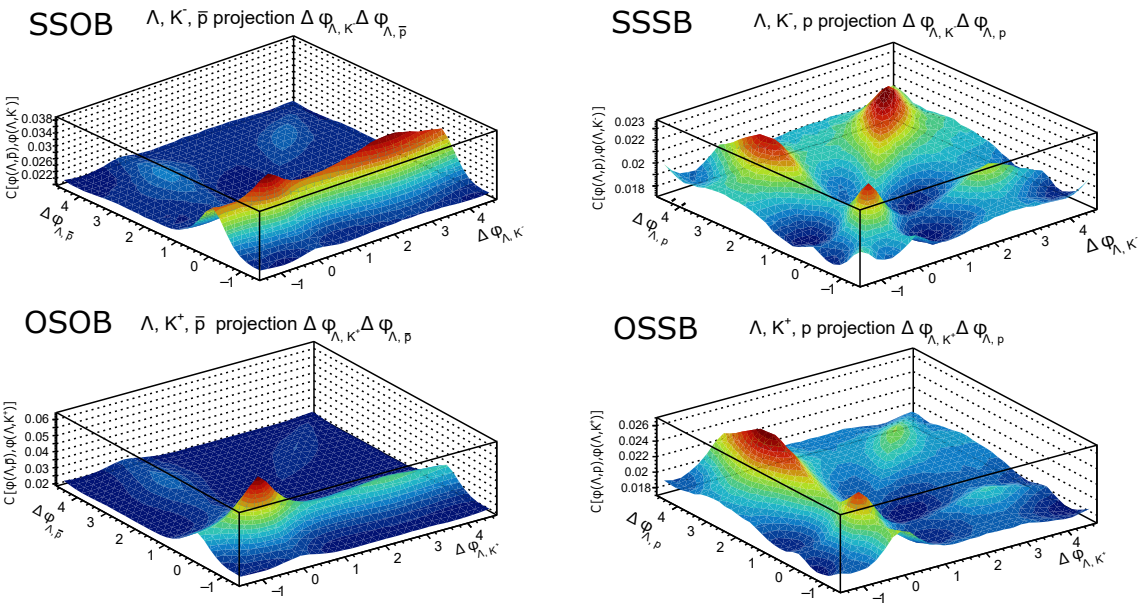

Figure 11: Three-Particle Correlations for all quantum number combiantions, projected onto $\Delta\phi_{12}$ versus $\Delta\phi_{13}$, default LSM.

The normalization correction from Eq.2 was made according to Eq. 3. Given this, the counts seen on the vertical axis represent the amount of times the given Kp pair is seen with respect to the total $\Lambda + \bar{\Lambda}$ particles that appear across events. This in turn yields comparable results across the four triplet pairs. The peaks observed at $\Delta\phi = 0$ look like particle production in the same jet, while the ones observed at $\Delta\phi$ look like particle production in the back to back jets.

SSOB: In figure 11 top left, the triplet of same strange and opposite baryon number is displayed in terms of the $\Delta\phi$ correlations. It can be interpreted that independently of the relative position between $\Lambda(\bar{\Lambda})$ and $K^+(K^-)$, there is a tendency for the $\Lambda(\bar{\Lambda})$ and $\bar{p}(p)$ to be close in the azimuthal angle. Within this tendency, there is a predilection towards $\Delta\phi_{\Lambda,K^-} = 0, \pi$.

SSSB: For same strange same baryon, top right in the same figure, there is overall a tendency for $\Delta\phi = 0, \pi$ between $\Lambda(\bar{\Lambda})$ and $p(\bar{p})$, as well as for $\Lambda(\bar{\Lambda})$ and $K^+(K^-)$, either independently of each other or with both $\Delta\phi$ being relatively similar.

OSSB: For opposite strange and same baryon number, figure 11 bottom right, it can be seen that there is a larger predilection for, independently of where the $\Lambda(\bar{\Lambda})$ and $p(\bar{p})$ are located with respect to one another, $\Lambda(\bar{\Lambda})$ and $K^+(K^-)$ to be close together. Nonetheless, a predilection is still kept for $\Delta\phi = 0, \pi$ for both cases.

OSOB: Lastly, bottom left, it is observed that $\Lambda(\bar{\Lambda})$ and $\bar{p}(p)$ have a very strong tendency to be at 0 degrees from each other while the same is true for $\Lambda(\bar{\Lambda})$ and $K^+(K^-)$, and also a significantly high tendency to be close independently of the relative position between $\Lambda(\bar{\Lambda})$ and $K^+(K^-)$. Nevertheless, there are still tendencies for the same situation with inverted roles between $\Delta\phi_{\Lambda,K+}$ and $\Delta\phi_{\Lambda,\bar{p}}$, as well as a smaller but present tendency for $\Delta\phi_{\Lambda,K+} \approx \Delta\phi_{\Lambda,\bar{p}}$. While this tendency seems at first glance insignificant,

due to the magnitude of the proportion of occurrences with respect to amount of Λs, it is comparable to some of the maxima in the top left and bottom right histograms and thus worth a mention for later discussion.

The aforementioned correlations seen on the diagonal of the histograms, i.e not parallel to the axis, imply $\Delta\phi_{12} \approx \Delta\phi_{13}$. This means that for the particle 1, there is a particle 2 and a particle 3 at equal distances from particle 1. While these are angular differences, which could mean that the particles 2 and 3 are at the same distance but in different directions, the trend shows more prominently around 0 and π, which means that particles 2 and 3, protons and charged kaons in this case, are in both cases at a distance $\Delta\phi_{23} \approx 0$.

4.1.2 Junctions

In figure 12 the same four projections as in figure 11 can be seen, except this case is for the three-particle correlations of the particles produced with junctions enabled in PYTHIA8. Overall, there is a larger likelihood for most correlations to be observed, since junctions are likelier to produce more baryons.

SSOB: On the top left, the ridge seen in $\Delta\phi_{\Lambda\bar{p}}$ has more distinct peaks where $\Delta\phi_{\Lambda,K^-} = 0, \pi$, while at the same time there is a larger prevalence of the secondary ridges.

SSSB: For the top right, where one looks for p instead of $\bar{p}$, there is comparatively a lesser chance to find the proton near the Λ while the kaon is back to back with both of them. However even this correlation is comparatively larger than in the no-junctions case.

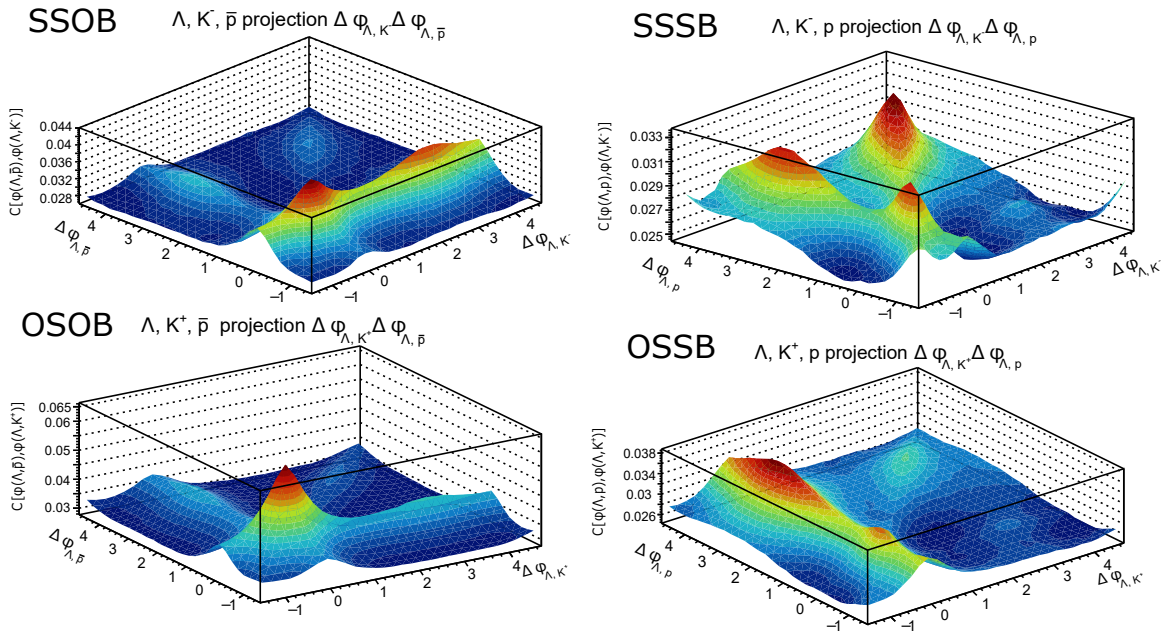

Figure 12: Three-Particle Correlations for all quantum number combiantions, projected onto $\Delta\phi_{12}$ versus $\Delta\phi_{13}$, junctions enabled.

OSSB: On the bottom right, the minima are comparable to the maxima in the no junction case for the given Λ, K^+, p correlation. Within the junction histogram, there is a

less prevalent peak for $(\Delta\phi_{\Lambda,p}, \Delta\phi_{\Lambda,K^-}) = (0, \pi)$, similarly to the top right case.

OSOB: Lastly, the correlation that is of most interest on the bottom left, shows similar maxima to the no junctions case, while the minima are larger, yielding in a lesser difference between maxima and minima.

4.1.3 Overall picture

Looking at both figures 11 and 12, when the triplets have opposite baryon number, $\Lambda(\bar{\Lambda}), \bar{p}(p)$ (left column), both baryons tend to be close in ϕ, while this is more prevalent in the no-junction case. Overall, the underlying tendency is for either the proton or the kaon to be close to the Λ baryon, while the remaining particle is somewhat more often close to the previous two. When the balancing strangeness $K^+(K^-)$ (bottom) is taken into account, there is a larger preference for the kaon to be also close to the baryons than anywhere else. If the meson has the same strange quantum number to the strange baryon $K^-(K^+)$ (bottom), there is no larger tendency for it to be close to the baryons.

On the other hand, if the second baryon has the same baryon number such that the pair is $\Lambda(\bar{\Lambda}), p(\bar{p})$ (right column) the underlying tendencies are for at least two of the particles to be 0 degrees apart in ϕ, while the third one is either close as well or back to back. If the balancing strangeness is present $K^+(K^-)$ as the third particle (bottom), the strange hadrons tend to be close together while the proton is either also close or, more likely, approximately back to back. However, if the strangeness is not balanced $K^-(K^+)$ (top), there is not such a large difference in the possible locations of the meson. It is however notable that independently on the meson's strangeness quantum number, there is a lesser tendency for it to be back to back to both Λ and proton, while this is more visible within the junctions.

Given what is known about the string models used for particle generation in this thesis, one expects balancing strangeness and baryon number to be, to different degrees, either close-by or back to back. While this behaviour is seen in the three-particle correlations discussed above, it is not the obvious which behaviours are due to a true correlation of opposite strangeness or baryon number, and which values are over-represented by correlations of particles that do not result from the same string breaking or process. This is why we need the Balance Function.

4.2 Three particle correlations: $\Delta\eta_{12}$ vs. $\Delta\eta_{13}$

4.2.1 Lund String Model method

In figure 13 the set of plots containing the $\Delta\eta_{12}$ versus $\Delta\eta_{13}$ projections of the three-particle correlations are presented.

SSOB: On the top left, the triplet $\Lambda K^-\bar{p}$ is represented in their $\Delta\eta$ correlations, where one can see that the Λ and $\bar{p}$ are close in $\Delta\eta$ independent of the position of the kaon. However, the least occuring scenarios for this triplet are of the same magnitude as the

highest occuring instances in the plot discussed below.

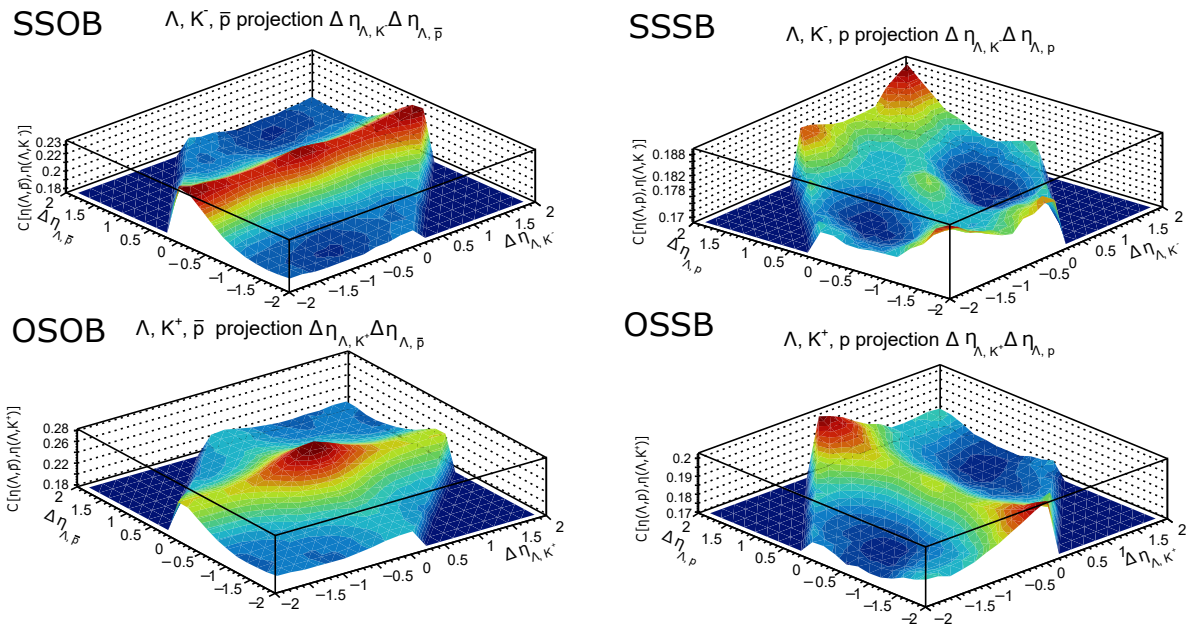

Figure 13: Three-Particle Correlations for all quantum number combiantions, projected onto $\Delta\eta_{12}$ versus $\Delta\eta_{13}$, default LSM.

SSSB: The correlation of the triplet $\Lambda K^- p$, seen in the top right, shows a hierarchy in predilection for given $\Delta\eta$ values. It is preferred by the kaon and proton to be both as far in pseudorapidity as one can see within the acceptance range. Alternatively, the proton should be far from both the Λ and the kaon which would be close together, in pseudorapidity. This is followed by some chance of finding the Λ, the proton and the kaon close together, and lastly, the kaon opposed to both Λ and proton.

OSSB: In the bottom right histogram for $\Lambda K^+ p$, the most likely is for the Λ and kaon to be located close to each other independently of where the proton is relative to the Λ. Nevertheless, the proton is opposed most often, followed by the chance of it being near to both Λ and kaon. The maximum likelihoods for this triplet is comparable to the average likelihood for the aforementioned triplet.

OSOB: Lastly, $\Lambda K^+ \bar{p}$ is seen in the bottom right. $\Lambda\bar{p}$ pairs have a strong predilection to be close in η independently of where the kaon is located, however the maximum is found when all three baryons are close in η.

4.2.2 Junctions method

In figure 14 the same projections as in the previous section in figure 13 are seen while now the particles produced by PYTHIA8 are done so with junctions enabled. Overall, the minima are higher than in the no-junctions case, in the same way as for the $\Delta\phi_{12}\Delta\phi_{13}$ projection.

SSOB: The top left figure shows predominantly the same preference for $\Lambda\bar{p}$ to be close in η, while the kaon is likelier to be also closer than in the no-junction case.

SSSB: In the top right figure there is a larger chance for all three $\Lambda K^- p$ to be close in pseudorapidity than for the baseline string model, making it comparatively as likely to the other cases discussed in the previous section.

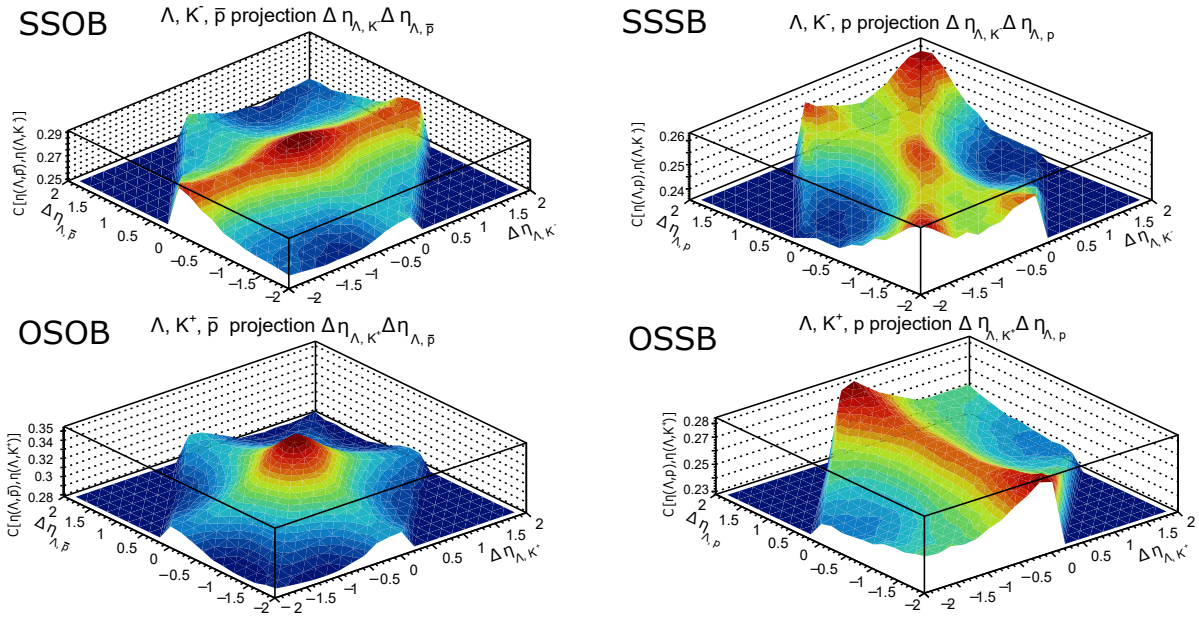

Figure 14: Three-Particle Correlations for all quantum number combiantions, projected onto $\Delta\eta_{12}$ versus $\Delta\eta_{13}$, junctions enabled.

OSSB: In the bottom right, there is now a similar likelihood for all particles to be close in η as for the strange hadrons to be close while the proton is back to back, while overall all cases are more likely to occur.

OSOB: When looking at the bottom left, with the triplet that is the main object of interest, one can observe that most of the probability is concentrated at $\Delta\eta_{\Lambda\bar{p}}, \Delta\eta_{\Lambda K^+} = (0, 0)$, while it is as likely for the Λ baryon to be close to any of the two other particles, which differs considerably from cases in the baseline PYTHIA8 model.

4.2.3 Overall picture

Looking at both figures 13 and 14, on the right-hand side where there is no balancing baryon number such that the two baryons are $\Lambda(\bar{\Lambda})$ and $p(\bar{p})$, there is generally no preference for where the baryons are located with respect to each other in pseudorapidity, showing a lack of correlation. When the balancing strangeness $K^+(K^-)$ is present (bottom), as opposed to the same strangeness (top), there is a tendency for the strange hadrons to be close in η.

When the baryon number is balanced such that the $\Lambda(\bar{\Lambda})$ and $\bar{p}(p)$ particles are part of the triplet, there is a general tendency for them to share similar momenta and thus be close in η. In the case of no balancing strangeness $K^-(K^+)$ (top), there is no apparent correlation between the strange hadrons. If balancing strangeness is also found in the

triplet $K^+(K^-)$ (bottom), there is a larger tendency for the meson to be close to both baryons than anywhere else, while this is more apparent in the junction case. The larger difference is that it is equally as common for any of the balancing particles to be close to the Λ baryon in the junctions case, while it is more common for the balancing anti-baryon than the balancing strangeness to be close to the Λ baryon in the baseline PYTHIA8 case.

From the aforementioned string and junction models, there is an overall expectation for all three particles $\Lambda\bar{p}K^+(\bar{\Lambda}pK^-)$ to be close in η when all three particles are produced from the same string(s), while this is perhaps more prevalent for the junction model. To which extent, it is so far not clear. There is a chance for the strange meson to be left with a smaller momentum fraction with respect to the two baryons in the simplest case of the Lund string model PYTHIA8 implementation. However it is not clear if the simplest model is the dominant one, or if it is instead completely dominated by the colour string alternative, or popcorn model. On the other hand there is a general expectation for the proton and kaon to be closer in momentum. From these projections it is not evident which process are dominating. So far, all correlations have given information that agrees with the predictions, but don't yield much new information. However, it is of relevance to have discussed them in detail in order to comprehend the implications of the following results, where the Balance Function is generated.

4.3 Balance Function

4.3.1 Lund String Model method

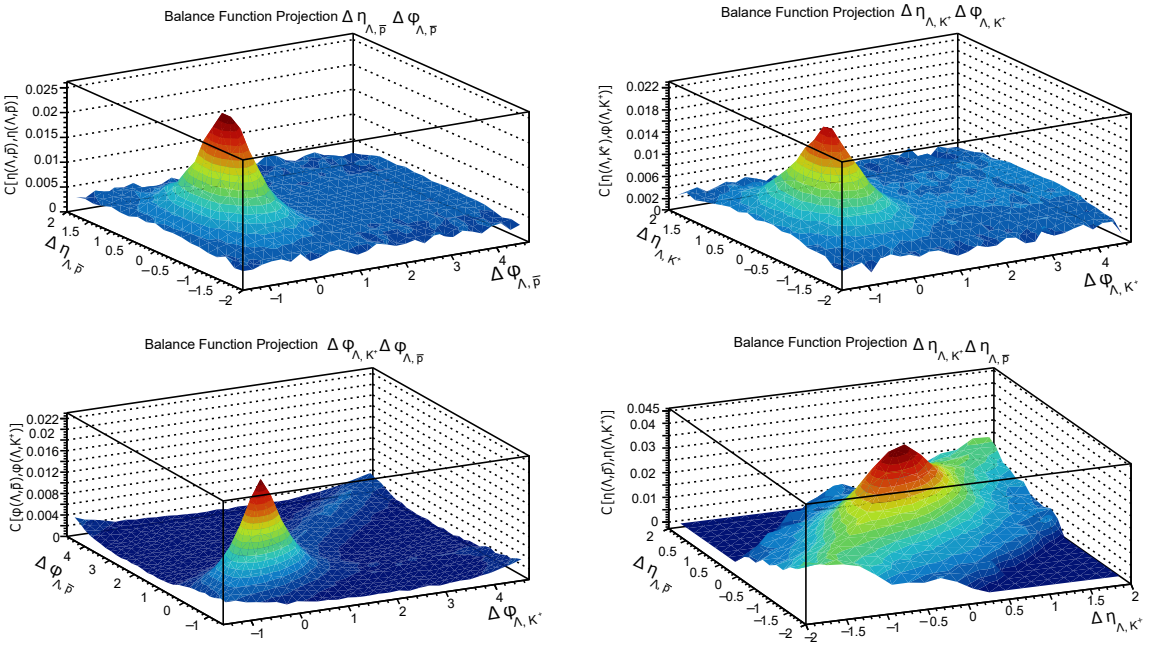

Figure 15: Balance Function, top projections corresponding to two-particle correlations for baryons (left) and strange hadrons (right); bottom projections corresponding to $\Delta\phi_{\Lambda K^+}$, $\Delta\phi_{\Lambda\bar{p}}$ (left) and $\Delta\eta_{\Lambda K^+}$ $\Delta\eta_{\Lambda\bar{p}}$ (right) projections. Default LSM.

In figure 15 top right, the Balance Function shows a strong predilection for Λ and K^+ to be close in ϕ and in pseudorapidity. The same can be said from figure 15 top left, between Λ and $\bar{p}$, while the correlation seems stronger. The predilection for closeness in the azimuthal angle and η is also observed in figure 15 bottom left and bottom right. Moreover, they show that the angular differences between Λ and K^+ tend to coincide to the angular differences between Λ and $\bar{p}$, although mostly prevalent in ϕ.

As mentioned in section 4.1.1. it is expected for all three balancing particles to be nearby in pseudorapidity, while it is unclear how close or how often. There is a similar scenario in regards to the azimuthal angle. From the Balance Function, one can observe a clear picture of the three-particle correlations where all three particles $\Lambda K^+\bar{p}$ ($\bar{\Lambda}K^-p$) are originated from the process or string breaking. These results yield quantifiable results where background or non-interesting correlations have been removed. The minimum counts shown in the histograms reach 0, since after the balancing is done, one can expect every value above 0 to be considered a signal. This is more evident in the $\Delta\eta_{\Lambda\bar{p}}$ vs. $\Delta\eta_{\Lambda K^+}$, where the correlations at $\pm(2,-2)$ are at 0 by default since one can not observe simultaneously three particles with such η values in the range (-1,1).

In the $\Delta\phi_{\Lambda\bar{p}}\Delta\phi_{\Lambda K^+}$ projection -bottom left-, it can be seen that all three particles have a strong predilection to be close in ϕ, approximately at $|\Delta\phi| < 1$, while the only other possibility is that $K^+\bar{p}$ are still very close, independently of where the Λ baryon is. For the$\Delta\eta_{\Lambda\bar{p}}$ $\Delta\eta_{\Lambda K^+}$ projection, there is a visibly stronger correlation at (0,0) than anywhere else, however it is still highly likely to find other pseudorapidity correlations, more specifically where $K^+\bar{p}$ are close independently of the Λ.

From the PYTHIA8 string-breaking picture, one could not predict whether the balancing particles would prefer to sit back to back or close to the Λ baryon in ϕ. It is now clearly observed that the latter is the likeliest scenario. There was an expectation to observe closeness in η among the 3 particles. However, there was not a clear expectation on the secondary tendencies. It is observed through the Balance Function that it is more reasonable to expect $K^+\bar{p}$ near in η independently on the Λ baryon's momentum, yielding the popcorn model as the leading model used through PYTHIA8.

4.3.2 Junctions method

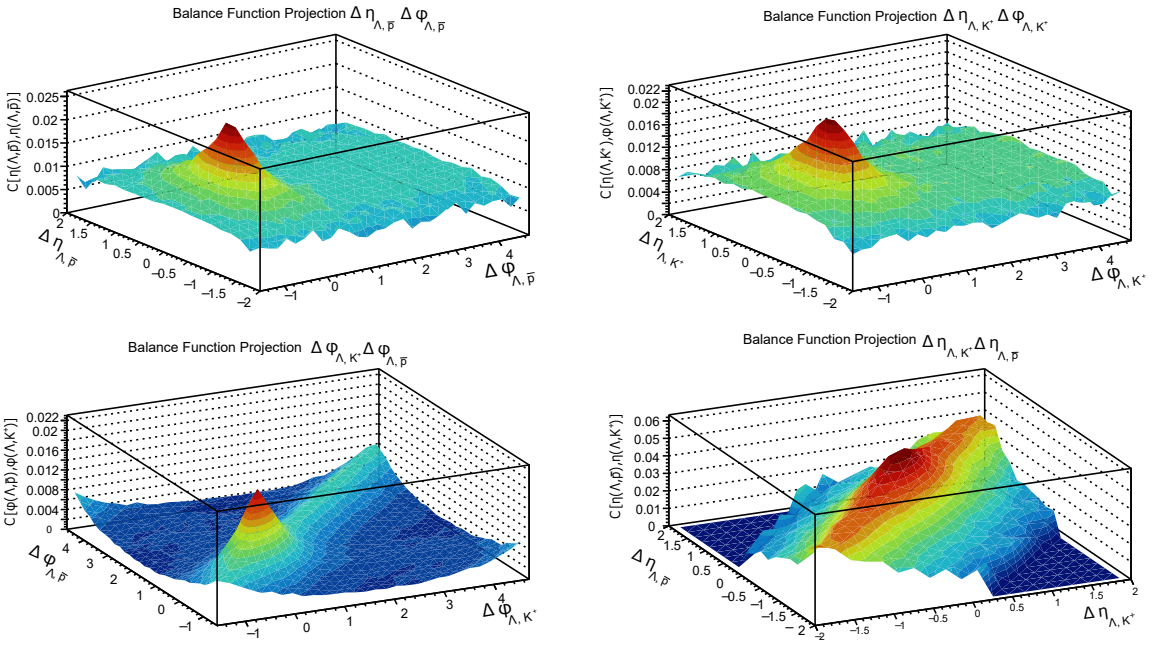

Figure 16: Balance Function, top projections corresponding to two-particle correlations for baryons (left) and strange hadrons (right); bottom projections corresponding to $\Delta\phi_{\Lambda K^+}$, $\Delta\phi_{\Lambda\bar{p}}$ (left) and $\Delta\eta_{\Lambda K^+}$ $\Delta\eta_{\Lambda\bar{p}}$ (right) projections. Junctions enabled.

The correlations in 16 look close to the ones for the no-junctions case in 15, except there is an overall more spread out set of probabilities. The top row figures become more relevant perhaps, since it can be seen that the effective correlations between the balancing particles and the trigger baryon are less restricted in η and $\Delta\phi$. Nonetheless, the projections which correlate all three particles at once, in $\Delta\phi$ (bottom left), and η (bottom right) set again a clear picture of how the selected particles are actually produced. While it is still true that above all options, the three particles like to be situated close along the beamline as well as with similar momenta, it is more likely than in the no-junction model for this not to be the case.

The $\Delta\phi_{\Lambda\bar{p}}\Delta\phi_{\Lambda K^+}$ projection shows that there is a larger independence on $\Lambda(\bar{\Lambda})$ as to where the balancing $K^+(K^-)$ and $\bar{p}(p)$ are located, as long as the latter two are closeby in ϕ. The $\Delta\eta_{\Lambda\bar{p}}\Delta\eta_{\Lambda K^+}$ projection shows largely the same behaviour, although more pronounced, where $K^+(K^-)$ and $\bar{p}(p)$ are close in η independently on $\Lambda(\bar{\Lambda})$, while it is still slightly favoured for all three particles to be close in η.

4.3.3 Overall picture

Independently on the model used, it remains true that the events which yield a $\Lambda(\bar{\Lambda})$ together with a balancing anti-baryon $\bar{p}(p)$ and strange meson $K^+(K^-)$, the likeliest is for the three particles to be found close in ϕ along the beamline, as well as in η and thus for the three particles to have similar momenta. The next likeliest alternative is for the balancing particles to be found close in ϕ or η, or both, independently of the $\Lambda(\bar{\Lambda})$

baryon's momentum-position values.

It is worth noting that there is four likely possible outcomes in this case: all particles close in ϕ and η, all particles close in η but only the balancing particles close in ϕ, only the balancing particles close in ϕ but all particles close in η, and only the balancing particles close in both ϕ and η.

Overall, the junction model is less restrictive in terms of the disparity between the likeliest and the next to likeliest scenario. However, the fact that both models yield similar tendencies despite some quantitative differences, indicates that there is a likelihood for these results to be able to be reproduced with experimental data, allowing for a mapping of strong interactions through three-particle correlations.

4.4 Comparative ranges

To study baryon number and strangeness production and collective behaviour, one can fix the balancing baryon number and ask where does that yield the balancing strangeness. This is the question asked within this section. The aim of defining a new observable to answer such question is not yet conclusive, such that the results shown here are yet to be curated into a more comprehensive picture.

4.4.1 Lund String Model method

In figure 17, four canvases with four plots each can be seen. These represent comparative amplitudes between a given range of $\Delta\phi$ and $\Delta\eta$ between the Λ and proton baryons corresponding to all 4 charge conjugate pairs of triplets. The left column sets $|\Delta\eta_{12}| < 0.2$ with particle 1 being the $\Lambda, \bar{\Lambda}$ baryon, and particle 2 being the second baryon $p, \bar{p}$. The right column does not set a range in $\Delta\eta_{12}$. The top row sets a range in $|\Delta\phi_{12} - \pi| < 0.3$ while the bottom column sets a range for $|\Delta\phi_{12}| < 0.3$. Next, the projections are taken for $\Delta\eta_{13}$ versus $\Delta\phi_{13}$ for all four possible combinations within the given range, and the normalisation described in section 3.1.2 is used.

The OSOB, SSSB, OSSB, SSOB acronyms are used for the discussion of these plots, and the main points of interest are $\Delta\phi_{13} = 0, \pi$.

Comparing OSOB with SSOB across the four canvases, it can be seen that if one peaks at one of the points of interest, the other one peaks at the other point of interest. If the range is set around π, between the opposite baryon number triplets, the opposite strangeness peaks also around π, while same strangeness peaks at 0. If the range is set around 0, OSOB peaks around 0 while SSOB peaks around π. Thus, opposite strangeness follows opposite baryon number yielding them all close in ϕ. For same baryon number, a similar behaviour is observed except this time it is the same strangeness that follows the same baryon number.

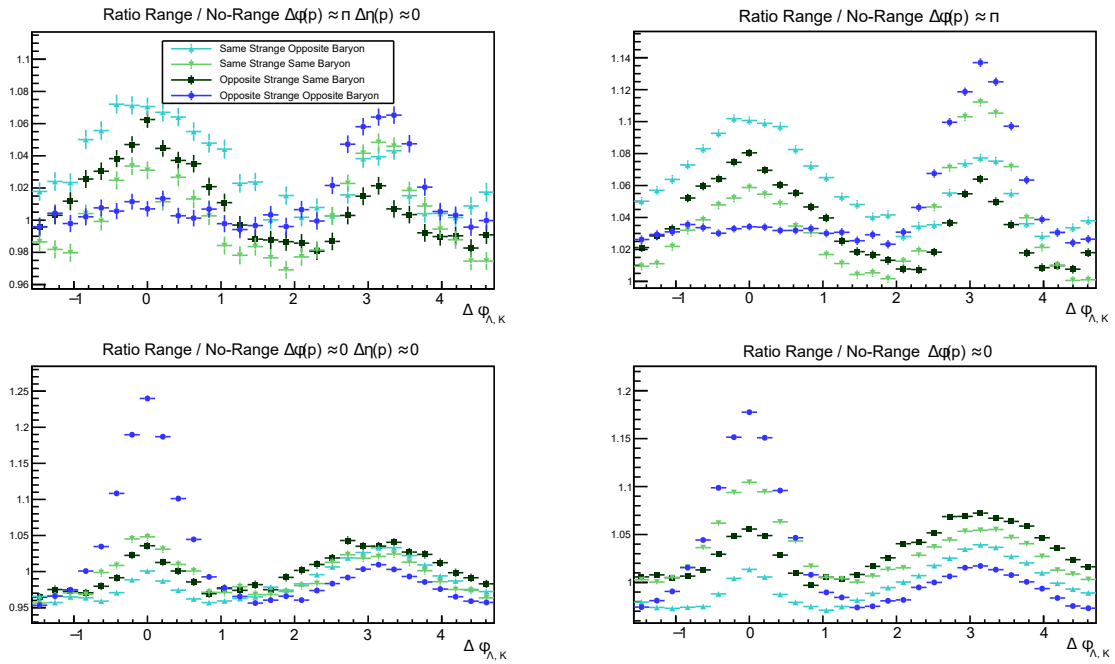

Figure 17: Ranges method as described above, applied on default LSM.

While these plots cannot yield quantitative estimations comparable to the BF, but rather a comparison of particle distributions for the different ranges, they are helpful for the understanding of the same concepts from a different point of view and testing whether the previously developed understanding through the use of the Balance Function still holds, and possibly shedding light on some new features. From the observation of these plots, it can be said that indeed when the balancing particles are correlated with the strange baryon, the strange meson will follow the balancing anti-baryon. At the same time, it is notably more re-occurring for all three particles to be close than for any other combination. Moreover, the tendency seems to be somewhat similar when the particles are completely uncorrelated, such that the uncorrelated baryon will be followed by the uncorrelated strange most often when back to back to the strange baryon, and no notable difference when close to the strange baryon. This confirms that while some features must be accounted for within a Balance Function, there is a clear signal standing out to the observer, which becomes more apparent thanks to the Balance Function.

4.4.2 Junctions method

Much of a similar behaviour is observed within the junctions model, in figure 18. The main distinction comes when comparing OSOB and SSSB, as it seems that there is not much of a difference between the maxima. However, these figures can only be understood through relative amplitudes, since the absolute magnitudes cannot give much information through the used methods. With this in mind, one can see that ratio between the maxima and minima within the OSOB bottom row plots is still larger than for the SSSB bottom row plots, which is the main interest point given that it is where one expects the larger correlation.

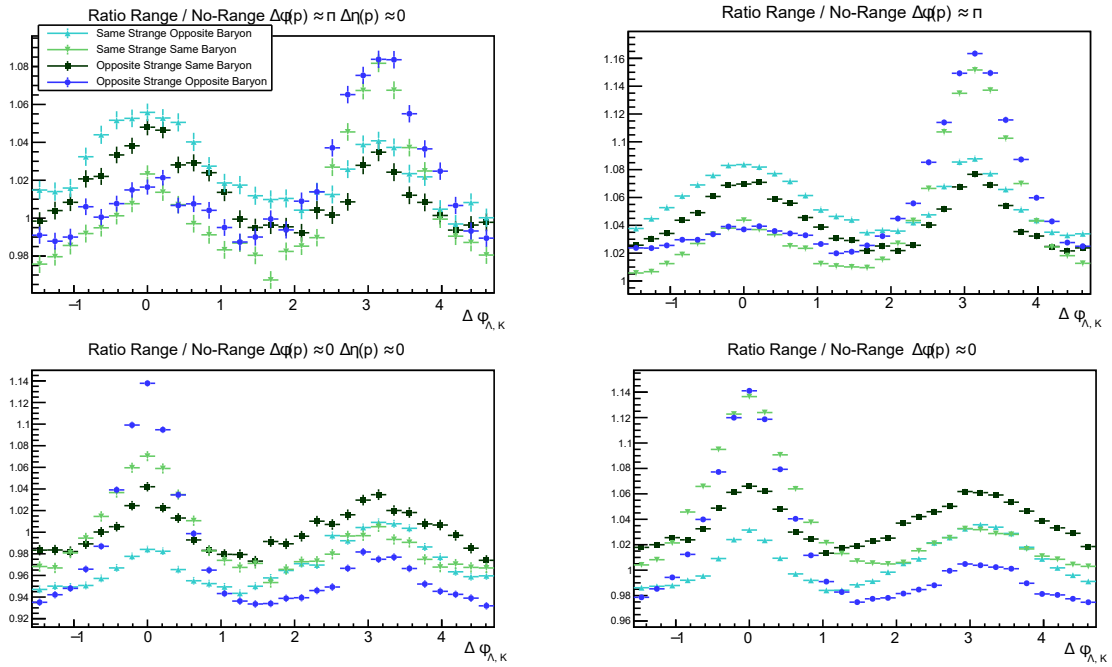

Figure 18: Ranges method as described above, applied on results with Junctions enabled.

4.4.3 Overall picture

The purpose of the comparative ranges perspective is partially to sanity check the Balance Function understanding, while at the same time attempting to observe any behaviours that are not apparent within the BF. One can see that the interpretation is overall the same, since in all cases the balancing strangeness and the balancing baryon number follows the $\Lambda(\bar{\Lambda})$ to a larger degree than for any other combinations. Therefore it is sensible to conclude that there is some underlying mechanism favoring this behaviour, at the very least in within the PYTHIA8 framework. Nevertheless, there is a notably similar behaviour, while not exactly the same, for the SSSB triplet within the junctions model, since it is the second triplet to stand out the most in this scenario when comparing amplitudes at the interest points $\Delta\phi_{13} = 0, \pi$ within the same plot.

This similarity for SSSB within junctions is not directly observed in the no-range three-particle correlations. However it can be inferred that the signal for the OSOB three particle correlation may be weaker given that a larger fraction of the apparent signal is composed by truly uncorrelated particles. This can be checked within the relative amplitudes between the OSOB and SSSB projections, both for no junctions and junction cases, in sections 4.1 and 4.2. This confirms the hypothesis, since there is a larger ratio of SSSB to OSOB signal for the junctions case.

5 Conclusions and Outlook

This thesis was aimed to model the correlations in the production of a strange baryon with a balancing anti-baryon and a balancing anti-strange meson with simulated data through the Monte Carlo based event generator PYTHIA8 in two configurations, the default Lund String Method, and with string junction enabled. This required the development

of three-particle correlations, in the momentum-space coordinate system η, ϕ. Such a novel method, so far majorly applied to two-particle correlations, presented challenges such as visualisation, interpretation of results and normalisation, as well as which triggering methods were used. A lack of in depth previous research using this method called for the tailoring from scratch of solutions to such challenges to the proposed problem. This has been successfully achieved through the use of tools such as ROOT histogram manipulation, where 4 dimensional histograms collected the correlations which sequentially were projected in groups of several 2 dimensional histograms through integration methods. The triggering methods followed from the simplest case examples used in two-particle correlations, as well as normalisation.

For the sake of interpretation, two viewpoints were adopted. On one hand, the making of a Balance Function to subtract the effects on the $\Lambda K^+\bar{p}(\bar{\Lambda}K^-p)$ correlations of the uncorrelated particles. On the other hand, ranges were set for the relative positions of the two baryons in η, ϕ in order to clearly observe the tendencies of the balancing meson in each of the given scenarios. The conclusions one can draw from these results is firstly, that there is indeed a general tendency to observe within the balancing triplets, or in other words, the production of these triplets and their momentum-space ordering, is not random. This ordering is found to be majorly a tendency of the truly correlated triplets to be close in ϕ and η. This of course is something highly dependant on the production mechanisms, and it is yet to be researched whether the behaviour would be the same with data taken through the ALICE detector.

The comparison of these three-particle correlations in models and in data will yield strong constraints on our understanding of particle production mechanisms. On one hand, it seems that from the two more prominent alternatives of production of such triplets within the LSM method, the more prominent one seems to be the closest scenario to the junctions model, where the meson is in between the two baryons. This meson in between has been empirically observed, which brings on the following point. In his doctoral thesis, J. Adolfsson, see [20], has shown that, while not completely hand in hand with empirical results in large systems where a QGP medium is present, the junctions variant of the Lund String Model implemented in PYTHIA8 comes ultimately very close to describing experimental data.

An immediate step to pursue as a continuation of this research would be to refine the ranges observable, such that they would allow for a clearer interpretation of the results.

In order to assure these suspected main hadronization processes are indeed dominating within the used frameworks, a prospective next step would look at whether the strange baryon $\Lambda(\bar{\Lambda})$ or the balancing meson $K^+(K^-)$ is found closer to the balancing anti-baryon $\bar{p}(p)$. From the discussions above, one would expect the kaon to be closest than the proton, given the ordering of the string breaking. Such a question would require a different approach for the three-particle correlations, where instead of correlating the balancing particles to the strange baryon, both strange particles should be correlated to the proton. Consequentially, within the BF, several small ranges in $\Delta\eta_{\bar{p}\Lambda}$ would be set, and compare the position of the peak in $\Delta\eta_{\bar{p}K^+}$ to the set range. If the peak is located at a smaller absolute value with respect to the set range, it would imply the kaon is closest to the proton, and thus indeed the main production mechanism is the one suspected from the

results of this thesis.

It is also interesting to check which combinations in $\Delta\eta_{12}, \Delta\eta_{13}, \Delta\phi_{12}$ and $\Delta\phi_{13}$ for the three particles are the likeliest within the Balance Function. As discussed in section 4.3.3, there are four such possibilities, but it has not yet been investigated which, if at all, is the predominant one.

Further work is suggested in order to increase the multiplicity of the simulated collisions to approach the multiplicities observed within heavy ion collisions. This would yield a baseline model where QGP is not considered, such that once it can be modelled in Monte Carlo simulations there will be a chance to compare the flow effects with and without QGP. In the long term, and with some additions to the observables defined in this thesis, one could eventually determine what fraction of the observed correlations are a signature of QGP, and what part can be explained by hadronisation processes already observed in proton-proton collisions.

6 References

[1] Alice Collaboration. "The ALICE experiment at the CERN LHC". In: *Journal of Instrumentation* 3.08 (Aug. 2008), S08002. DOI: 10.1088/1748-0221/3/08/S08002.

[2] B. R. Martin and G. Shaw. *Particle Physics: 6. The Quark Model*. Wiley, 2017. ISBN: 978-1-118-91216-4.

[3] *File:Standard Model of Elementary Particles.svg - Wikimedia Commons*. Online; accessed 4. Apr. 2023. Apr. 2023. URL: https://commons.wikimedia.org/wiki/File:Standard_Model_of_Elementary_Particles.svg.

[4] Contributors to Wikimedia projects. *Color charge - Wikipedia*. Online; accessed 4. Apr. 2023. Feb. 2023. URL: https://en.wikipedia.org/w/index.php?title=Color_charge&oldid=1138077958.

[5] B. R. Martin and G. Shaw. *Particle Physics: 7. QCD, jets and gluons*. Wiley, 2017. ISBN: 978-1-118-91216-4.

[6] ALICE Collaboration. "The ALICE experiment – A journey through QCD". In: *EPJ* (2022). eprint: arXiv:2211.04384[nucl-ex].

[7] A. Andronic et al. "Decoding the phase structure of QCD via particle production at high energy". In: *Nature* 561 (2018), pp. 321–330. DOI: 10.1038/s41586-018-0491-6. URL: https://doi.org/10.1038/s41586-018-0491-6.

[8] Jonah E. Bernhard, J. Scott Moreland, and Steffen A. Bass. "Bayesian estimation of the specific shear and bulk viscosity of quark-gluon plasma". In: *Nat. Phys.* 15 (Nov. 2019), pp. 1113–1117. ISSN: 1745-2481. DOI: 10.1038/s41567-019-0611-8.

[9] Wit Busza, Krishna Rajagopal, and Wilke van der Schee. "Heavy Ion Collisions: The Big Picture and the Big Questions". In: *Annual Review of Nuclear and Particle Science* 68.1 (2018), pp. 339–376. DOI: 10.1146/annurev-nucl-101917-020852. URL: https://doi.org/10.1146/annurev-nucl-101917-020852.

[10] CMS Collaboration. "Observation of Long-Range Near-Side Angular Correlations in Proton-Proton Collisions at the LHC". In: *arXiv* (Sept. 2010). DOI: 10.1007/JHEP09(2010)091. eprint: 1009.4122.

[11] James L. Nagle and William A. Zajc. "Small System Collectivity in Relativistic Hadronic and Nuclear Collisions". In: *Annual Review of Nuclear and Particle Science* 68.1 (2018), pp. 211–235. DOI: 10.1146/annurev-nucl-101916-123209. URL: https://doi.org/10.1146/annurev-nucl-101916-123209.

[12] Maria Vasileiou. "Identified charged hadron production in pp and Pb-Pb collisions with ALICE at the LHC". In: *EPJ Web of Conferences* 126 (Dec. 2015). DOI: 10.1051/epjconf/201612604052.

[13] R. L. Workman et al. "Review of Particle Physics". In: *PTEP* 2022 (2022), p. 083C01. DOI: 10.1093/ptep/ptac097.

[14] Bjorn S. Nilsen. "Heavy-flavor production in LHC pp interactions using the ALICE detector". In: *Nucl. Phys. Proc. Suppl* 233 (Oct. 2012), pp. 201–206. DOI: 10.1016/j.nuclphysbps.2012.12.077.

[15] Nicolò Jacazio. "PID performance of the ALICE-TOF detector in Run 2". In: *Proceedings of Science* (Sept. 2018). DOI: 10.48550/arXiv.1809.00574. eprint: 1809.00574.

[16] Christian Bierlich et. al. "A comprehensive guide to the physics and usage of PYTHIA 8.3". In: *SciPost Physics Codebases* (Mar. 2022), pp. 7–12. DOI: 10.48550/arXiv.2203.11601. eprint: 2203.11601.

[17] Christian Bierlich et. al. "A comprehensive guide to the physics and usage of PYTHIA 8.3". In: *SciPost Physics Codebases* (Mar. 2022), pp. 163–169. DOI: 10.48550/arXiv.2203.11601. eprint: 2203.11601.

[18] Šárka Todorova-Nová. "Baryon production in the quantized fragmentation of helical QCD string". In: *Phys. Rev. D* 104.3 (Aug. 2021), p. 034012. ISSN: 2470-0029. DOI: 10.1103/PhysRevD.104.034012.

[19] *ROOT: ROOT Reference Documentation.* Online; accessed 25. April 2023. May 2023. URL: https://root.cern/doc/v626.

[20] Jonatan Adolfsson. "Study of Ξ-Hadron Correlations in pp Collisions at $\sqrt{s}$ = 13 TeV Using the ALICE Detector". In: *Lund University* (2020). URL: https://portal.research.lu.se/en/publications/study-of-%CE%BE-hadron-correlations-in-pp-collisions-at-isi-13-tev-usi.

7 Appendix A: figures

7.1 Three Particle Correlations

7.1.1 Lund String Model

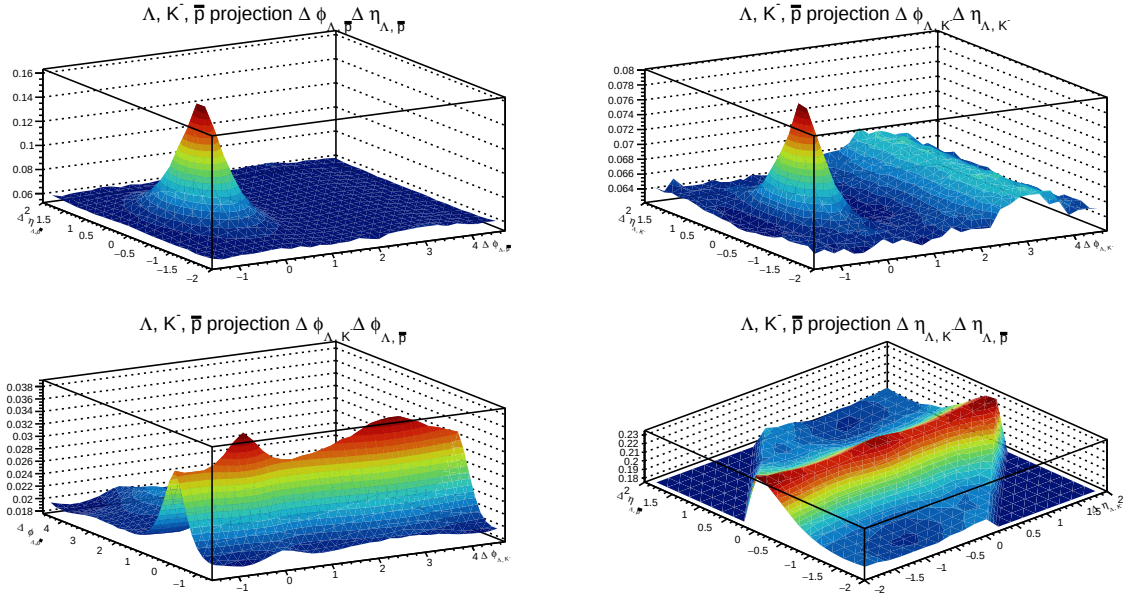

Figure 19: Three Particle Correlations SSOB, default LSM

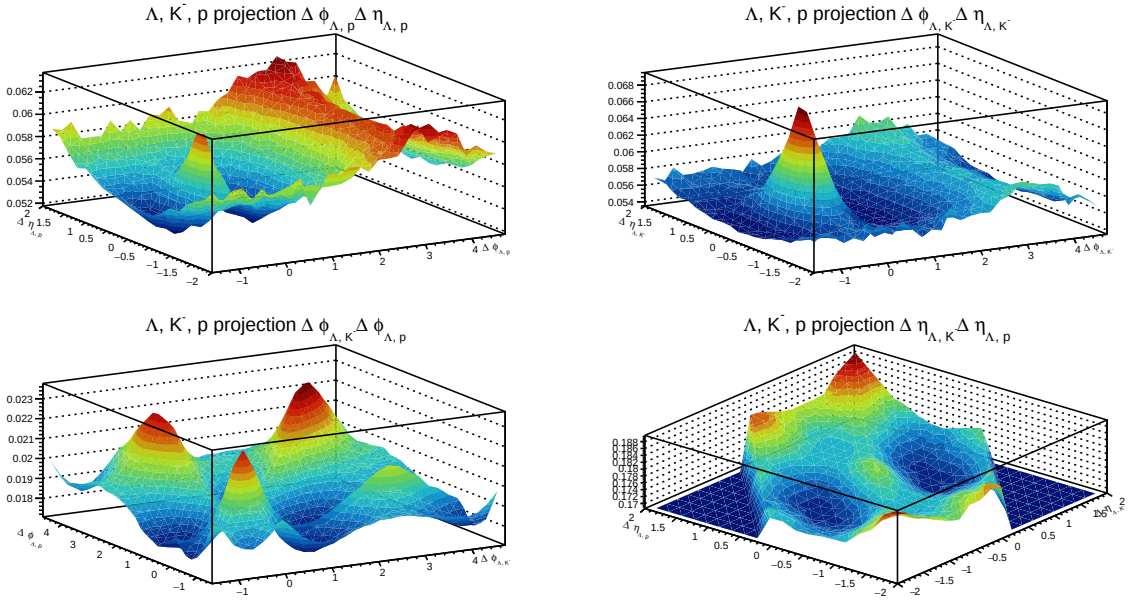

Figure 20: Three Particle Correlations SSSB, default LSM

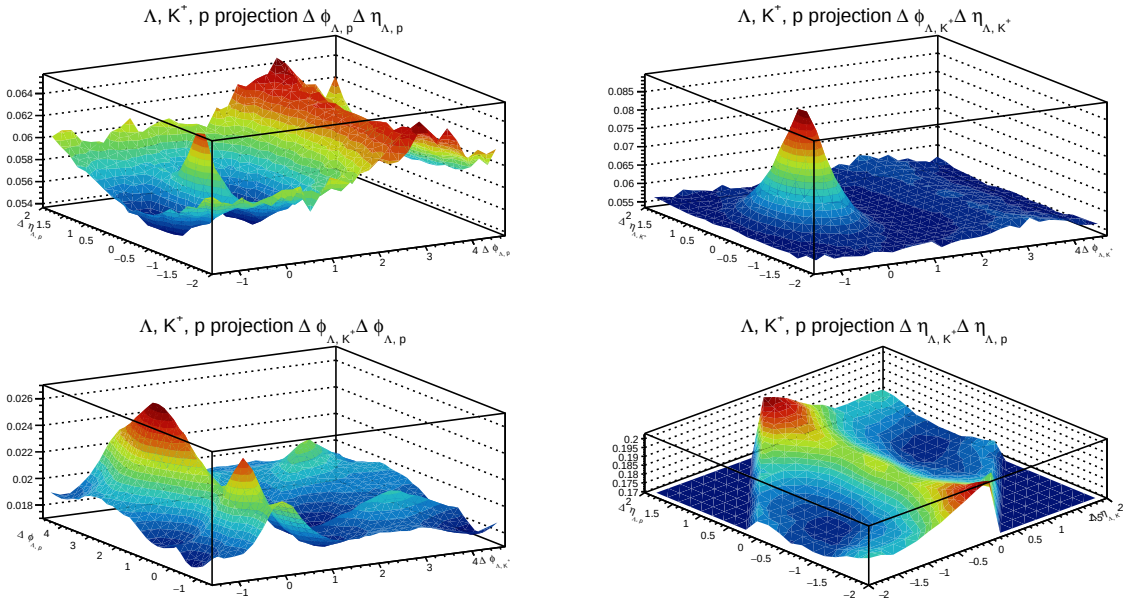

Figure 21: Three Particle Correlations OSSB, default LSM

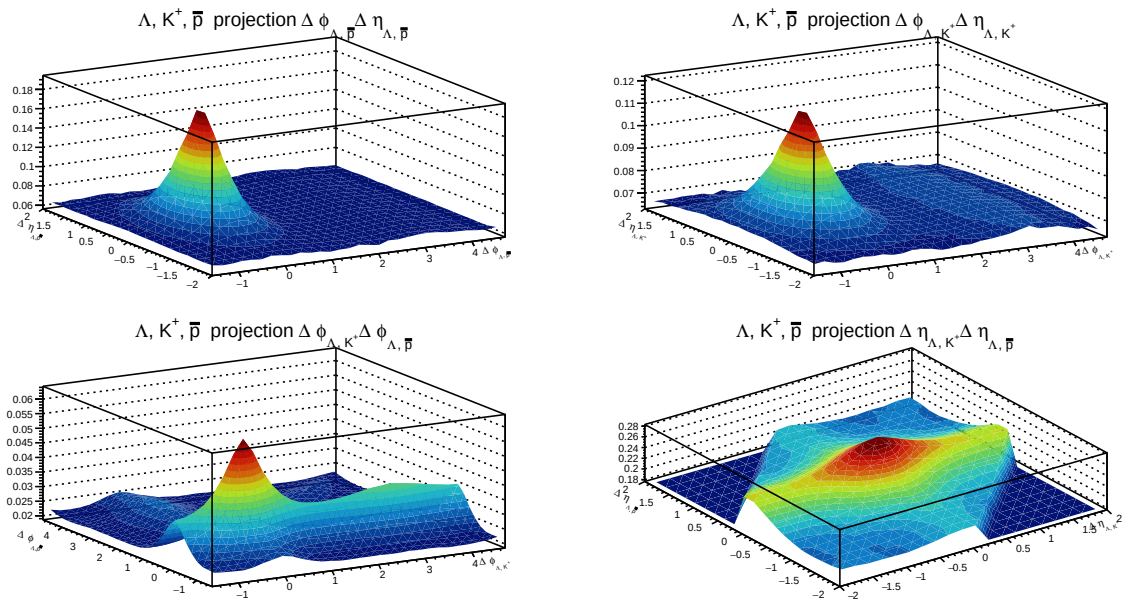

Figure 22: Three Particle Correlations OSOB, default LSM

7.1.2 Junctions

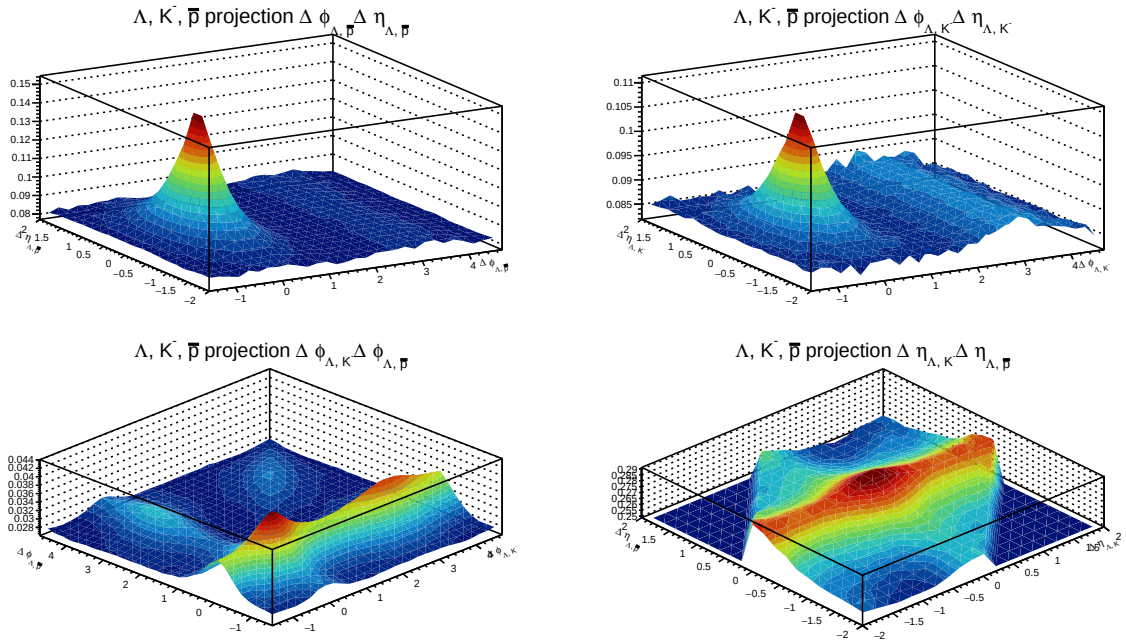

Figure 23: Three Particle Correlations SSOB, junctions enabled.

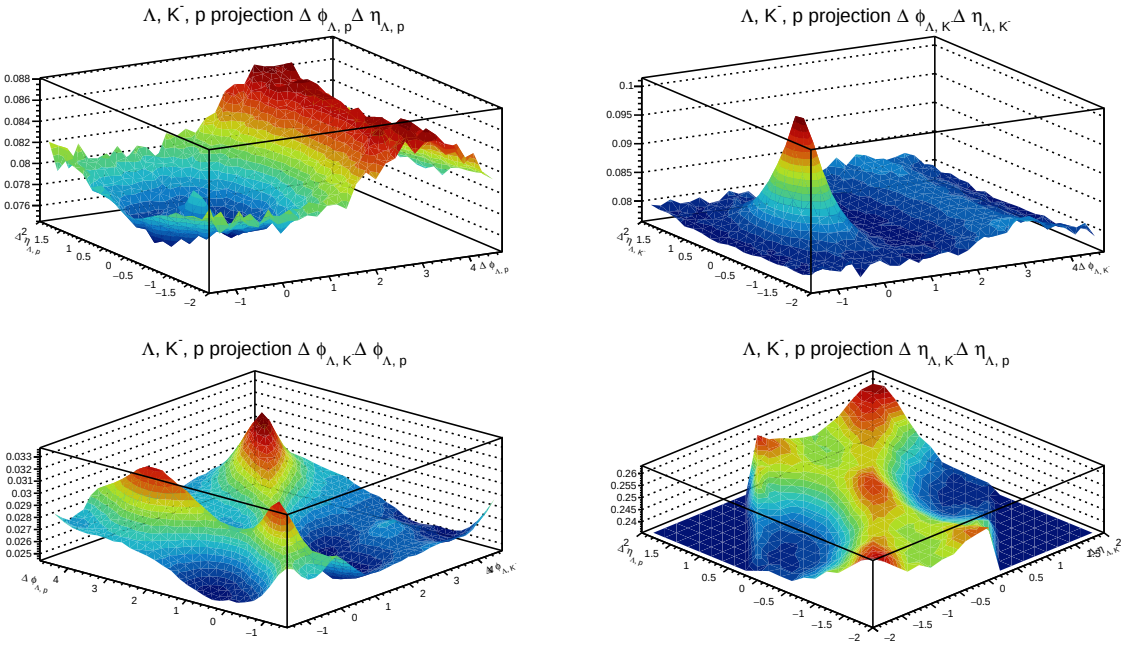

Figure 24: Three Particle Correlations SSSB, junctions enabled.

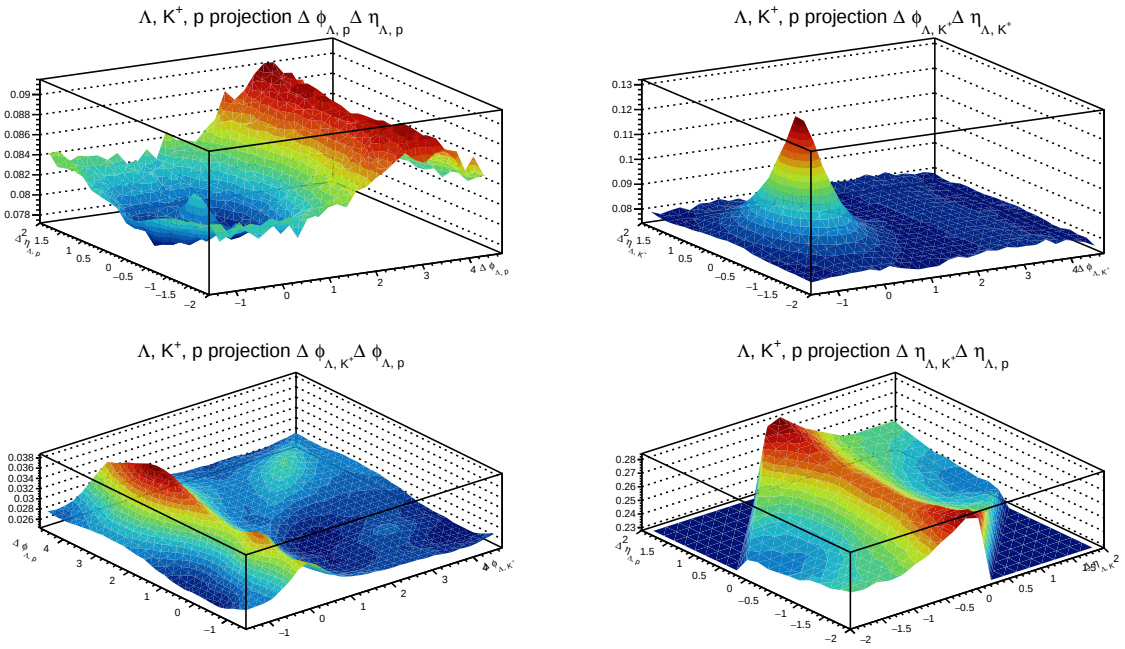

Figure 25: Three Particle Correlations OSSB, junctions enabled.

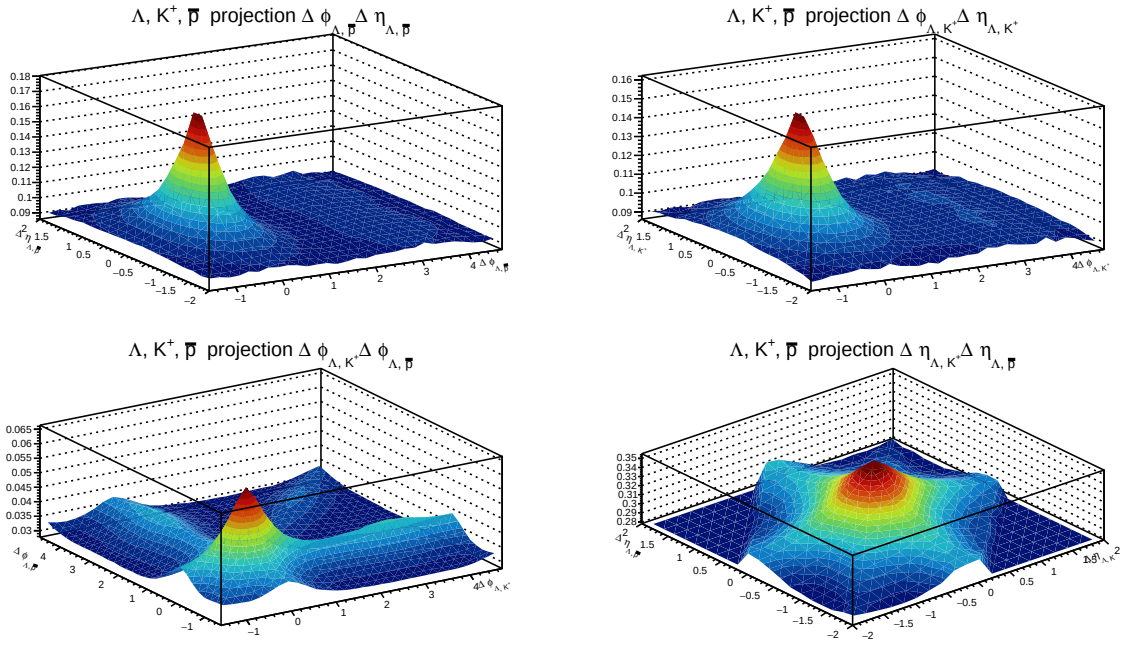

Figure 26: Three Particle Correlations OSOB, junctions enabled.

7.2 Ranges without ratios.

7.2.1 Lund String Model

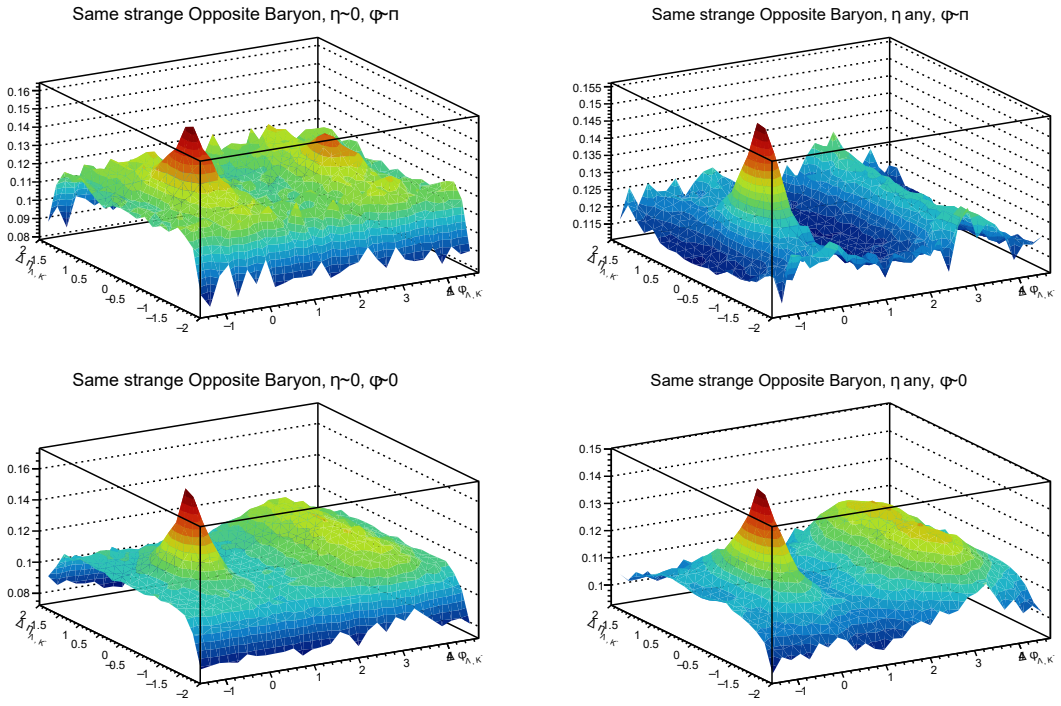

Figure 27: Ranges SSOB, default LSM

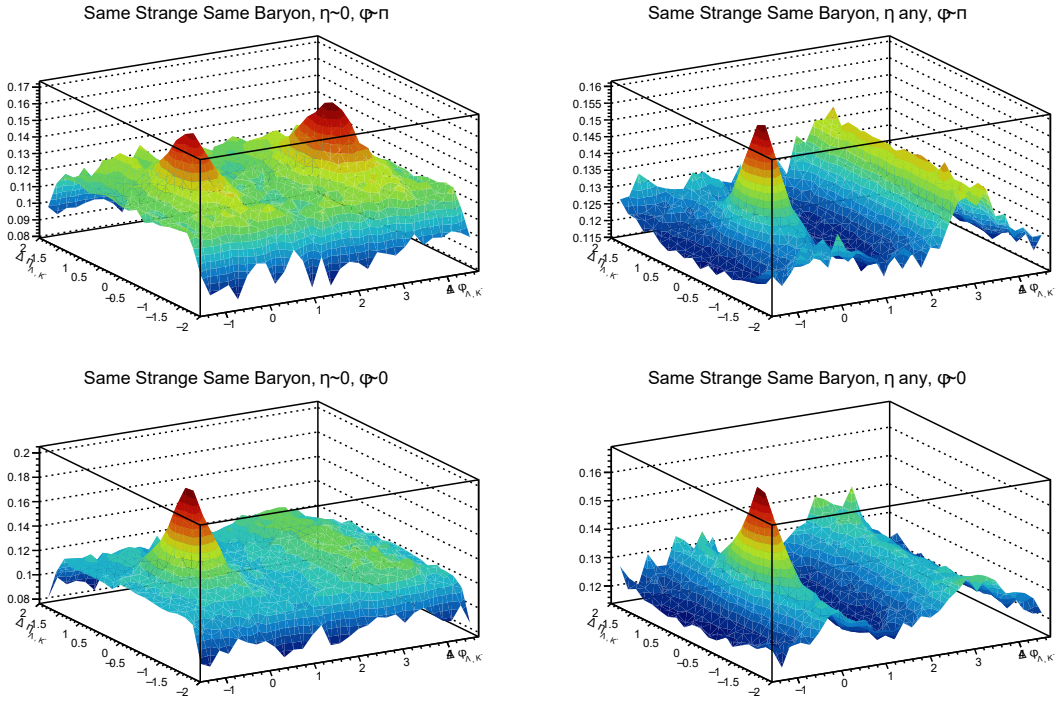

Figure 28: Ranges SSSB, default LSM

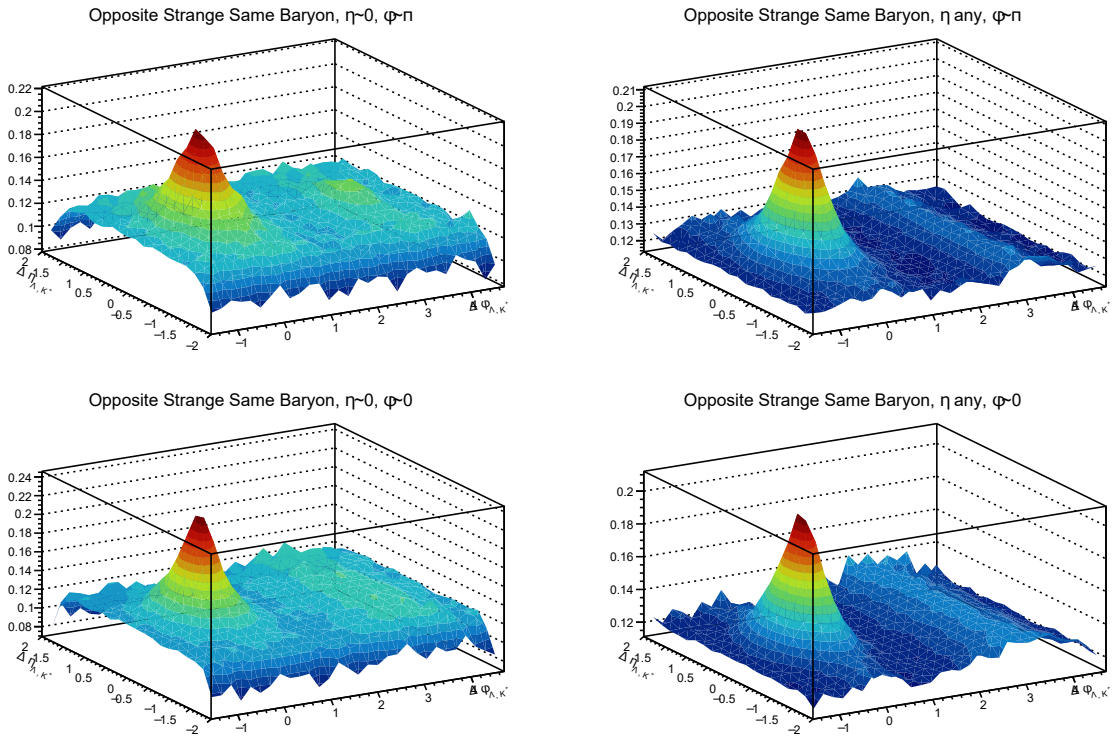

Figure 29: Ranges OSSB, default LSM

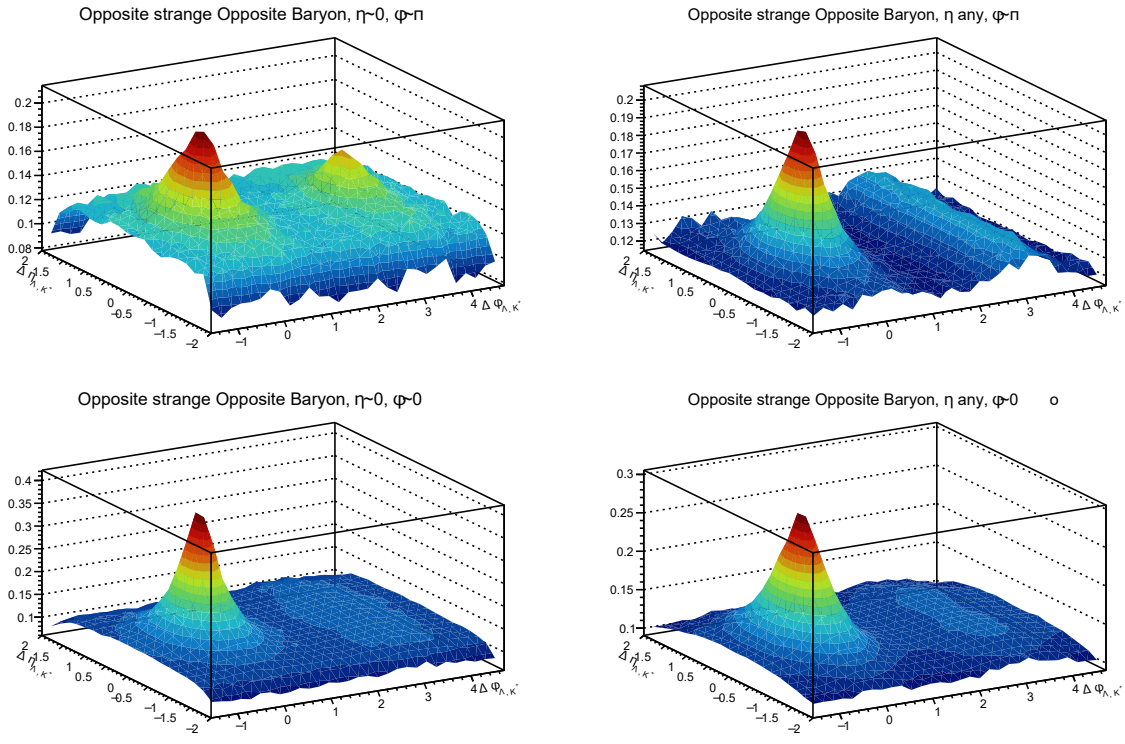

Figure 30: Ranges OSOB, default LSM

7.2.2 Junctions

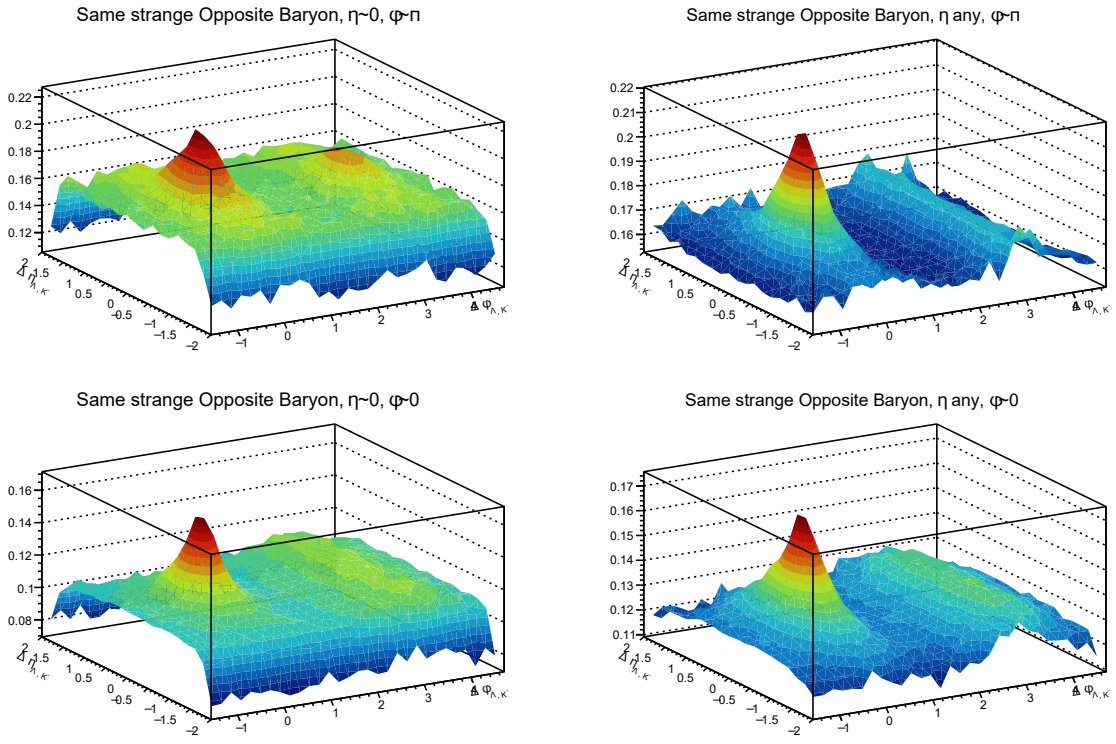

Figure 31: Ranges SSOB, junctions enabled.

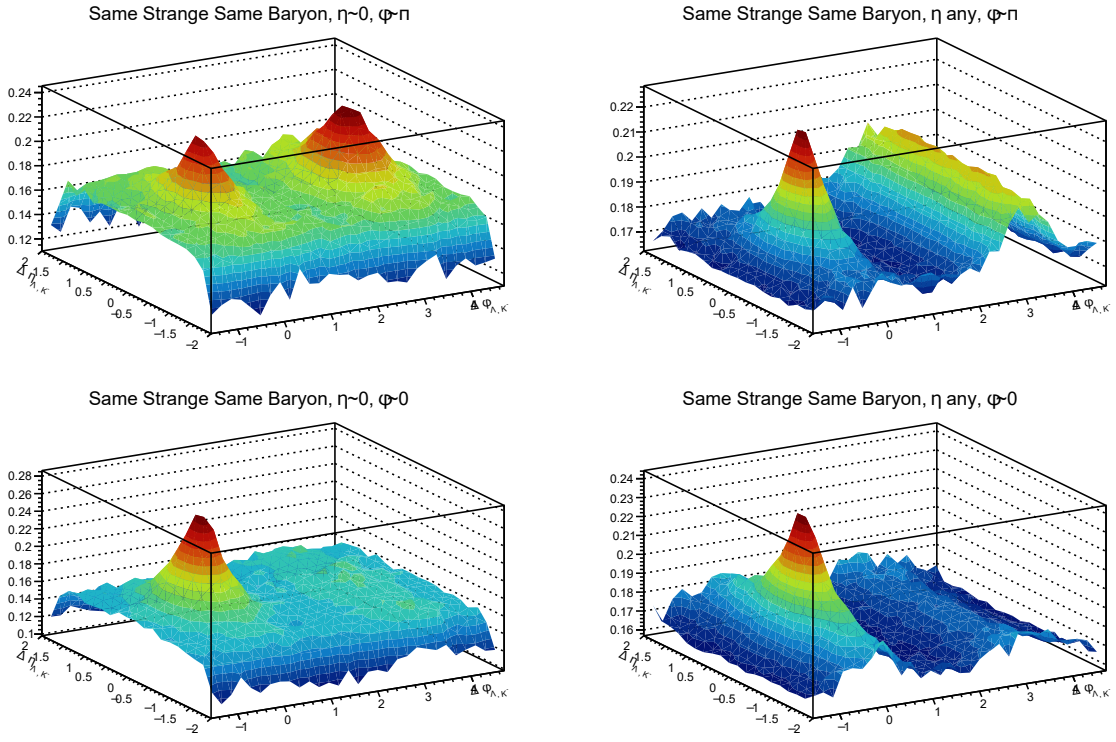

Figure 32: Ranges SSSB, junctions enabled.

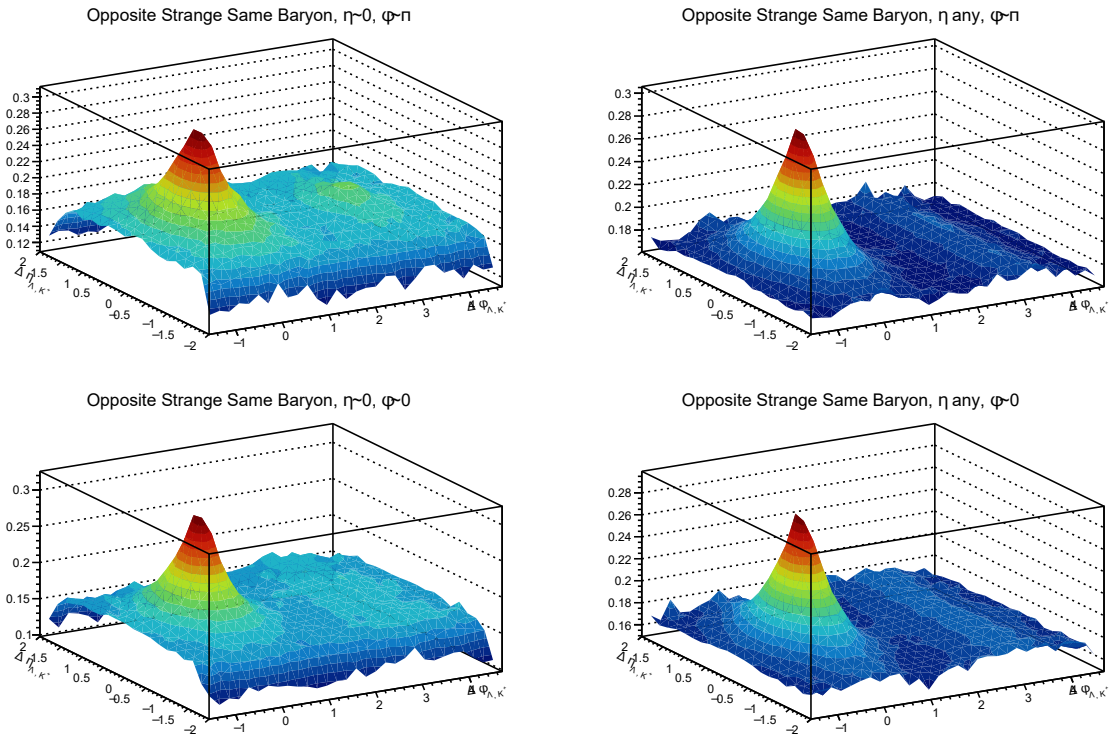

Figure 33: Ranges OSSB, junctions enabled.

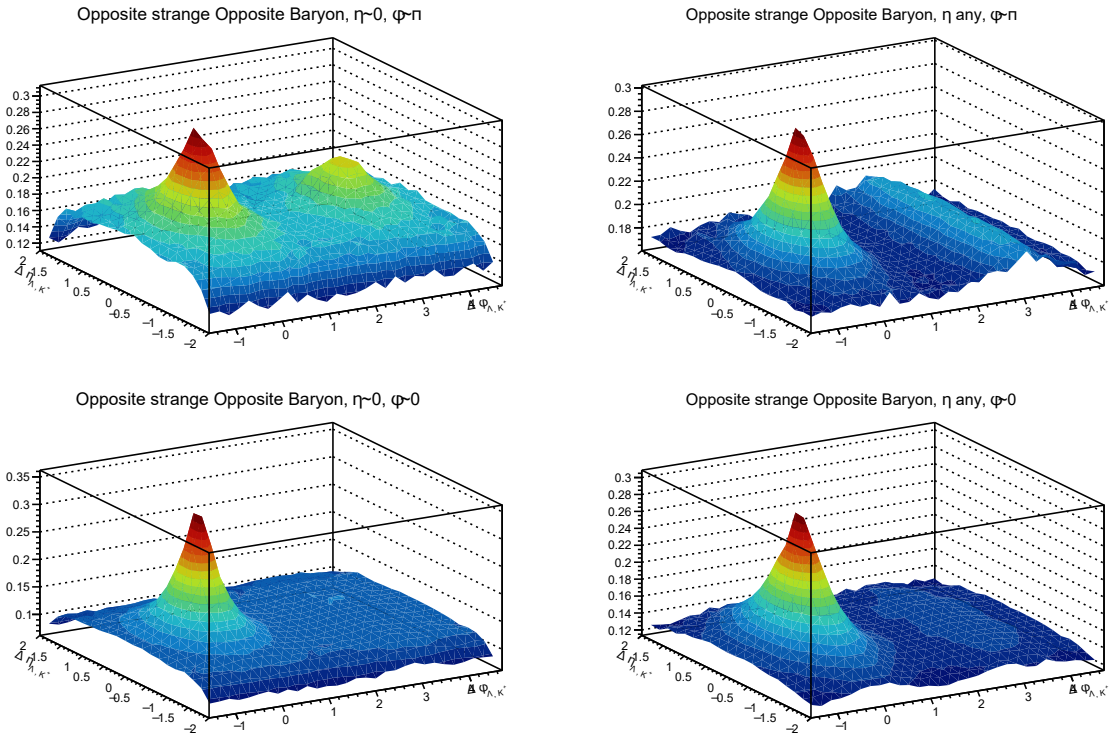

Figure 34: Ranges OSOB, junctions enabled.

7.3 Ranges with ratios.

7.3.1 Lund String Model

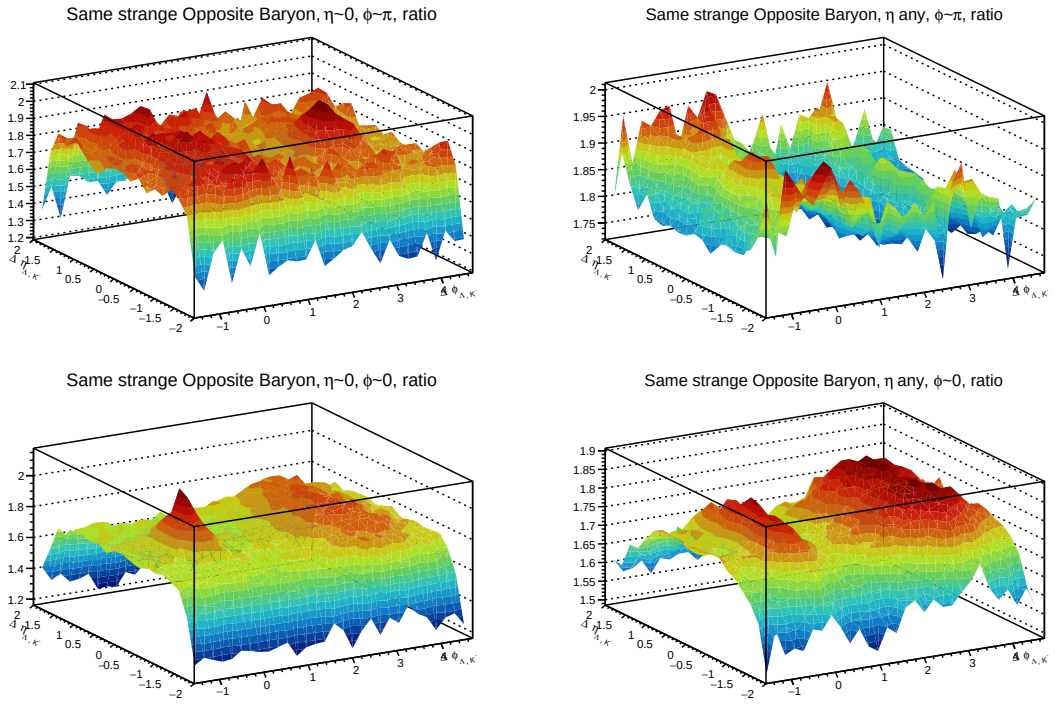

Figure 35: Ratios SSOB, default LSM

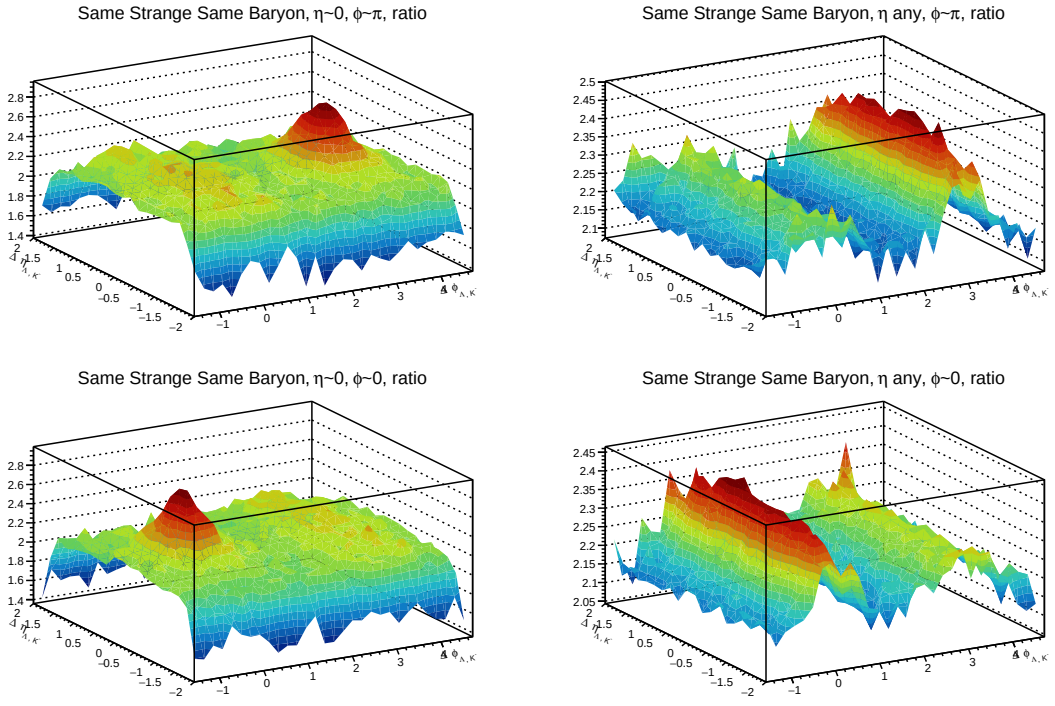

Figure 36: Ratios SSSB, default LSM

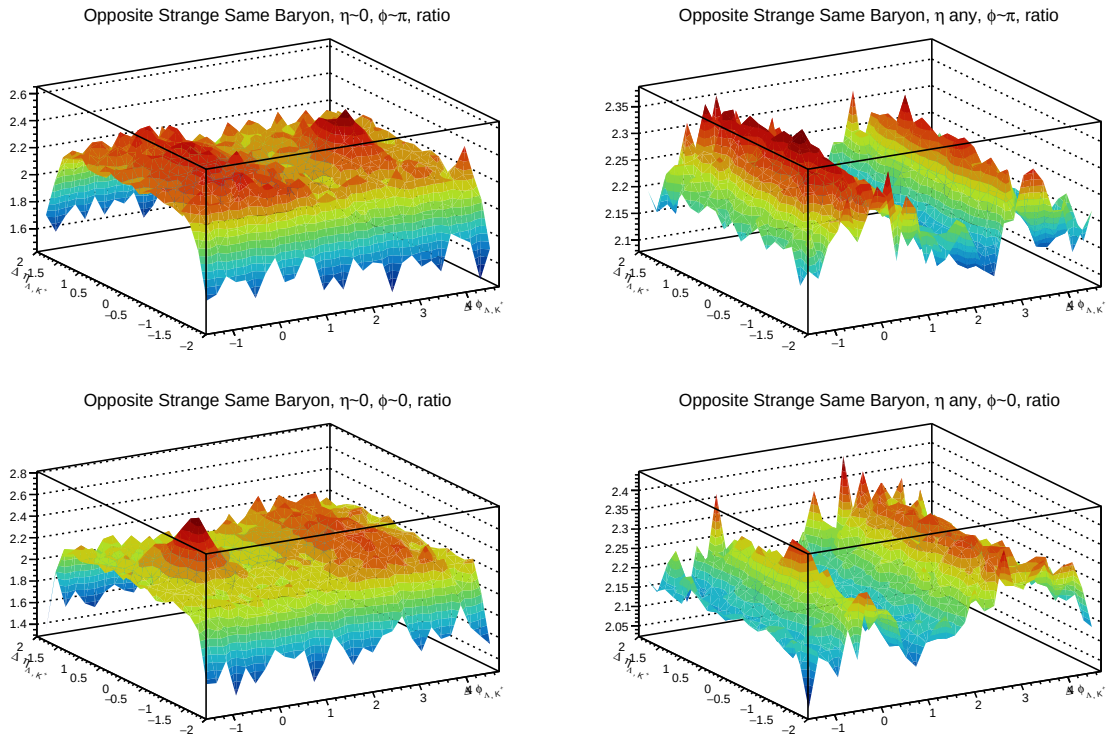

Figure 37: Ratios OSSB, default LSM

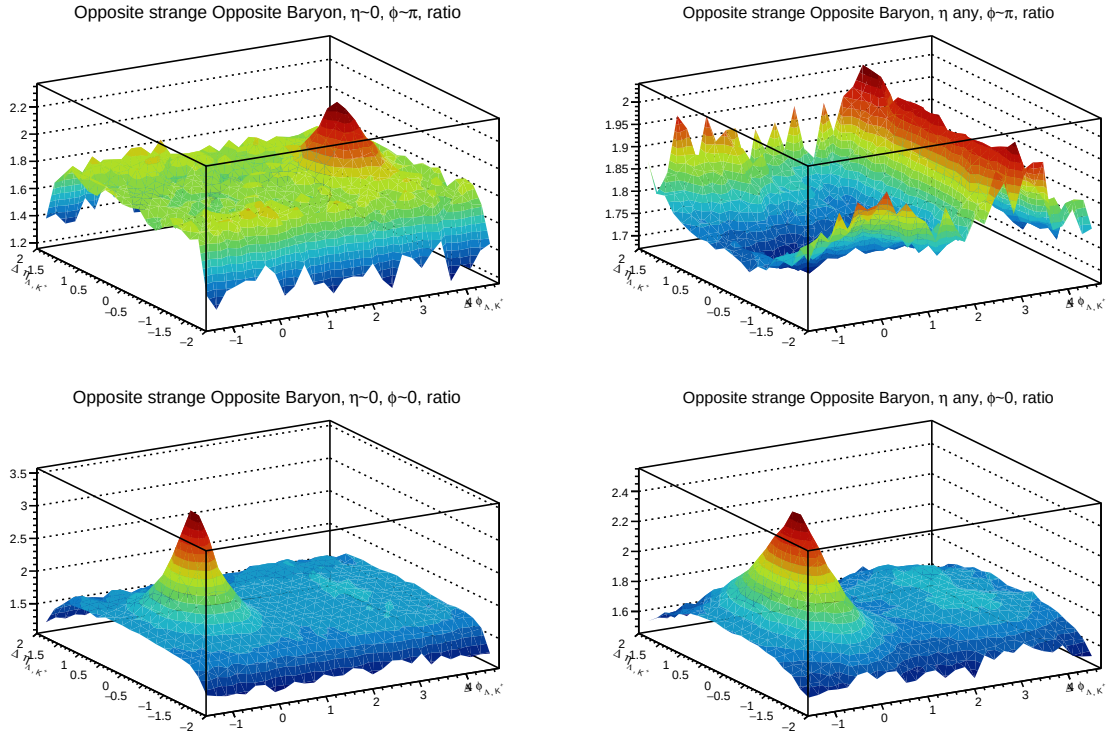

Figure 38: Ratios OSOB, default LSM

7.3.2 Junctions

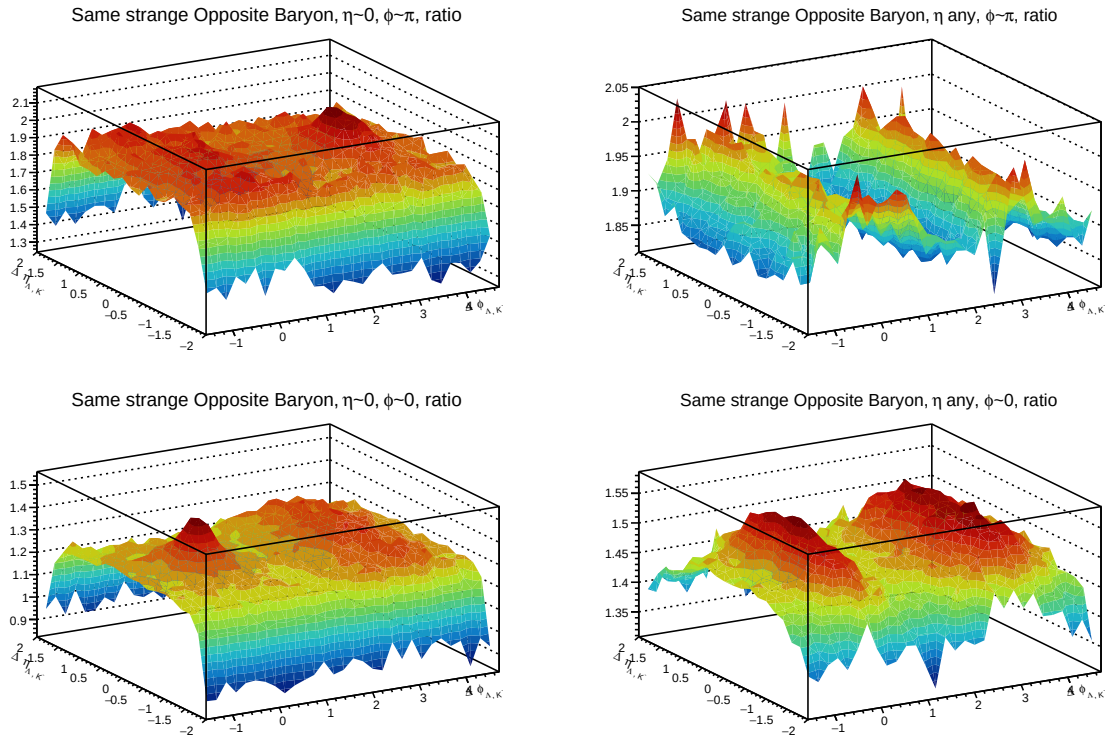

Figure 39: Ratios SSOB, junctions enabled.

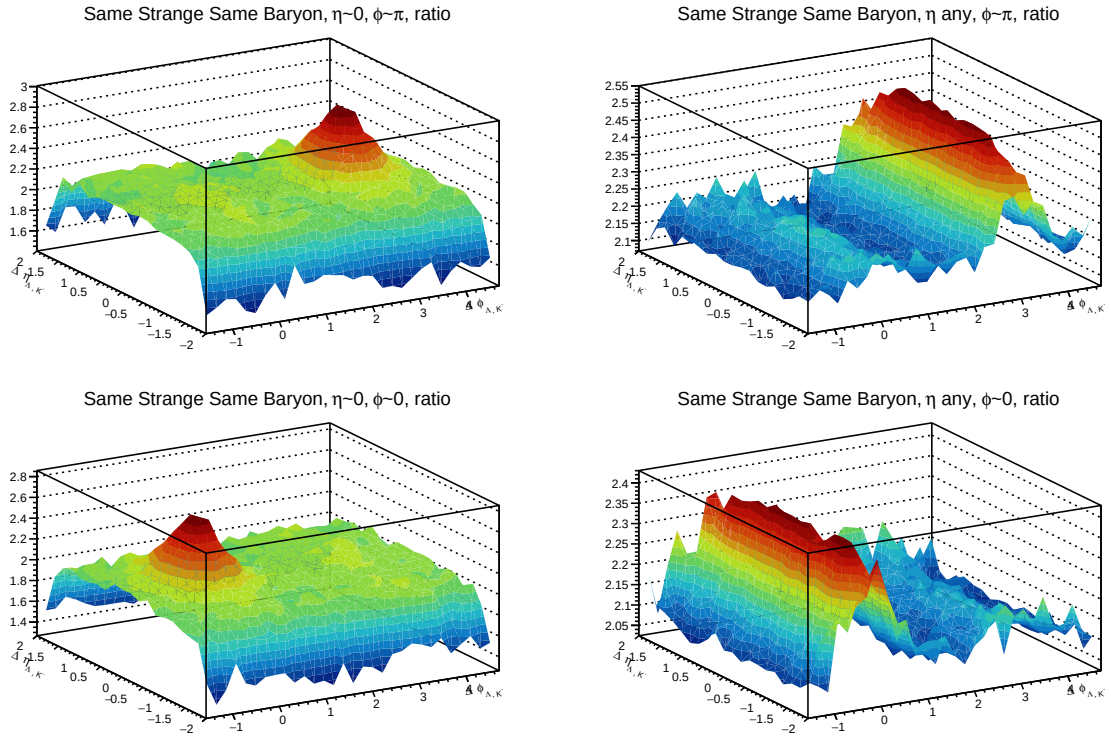

Figure 40: Ratios SSSB, junctions enabled.

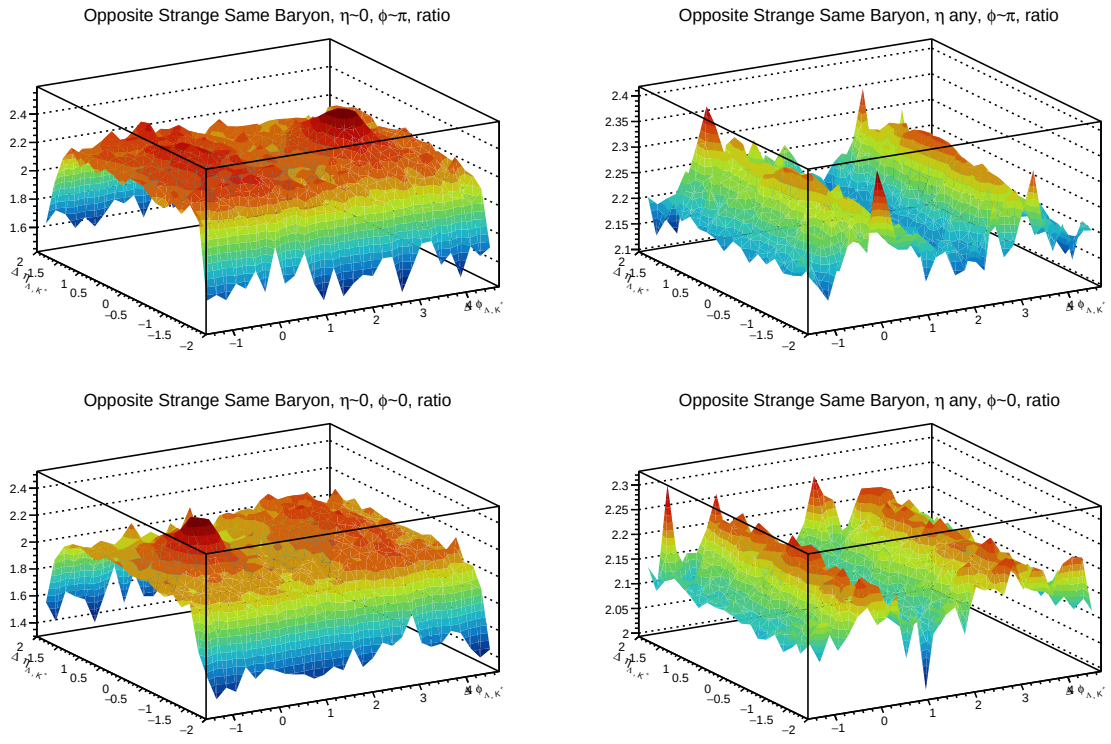

Figure 41: Ratios OSSB, junctions enabled.

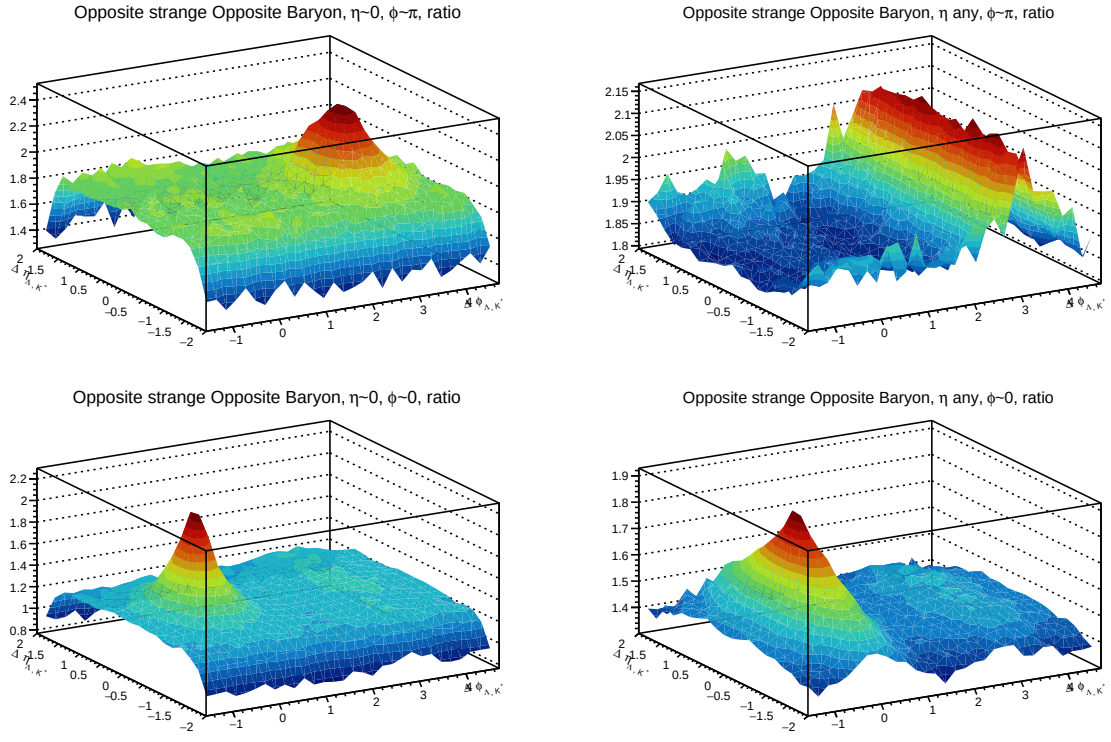

Figure 42: Ratios OSOB, junctions enabled.

8 Appendix B

Presented below is the code snipped configuring PYTHIA8 in order to enable junctions within LSM.

```
    pythia.readString("Beams:eCM = 13000."); // 13 TeV pp
pythia.readString("SoftQCD:nonDiffractive = on");

// junctions enabling from Christian Bierlich and Adrian Nassirpour,
 private communication.
if(kJunctions)
  {
    pythia.readString("MultiPartonInteractions:pT0Ref = 2.15");
    pythia.readString("BeamRemnants:remnantMode = 1");
    pythia.readString("BeamRemnants:saturation = 5");
    pythia.readString("ColourReconnection:mode = 1");
    pythia.readString("ColourReconnection:allowDoubleJunRem = off");
    pythia.readString("ColourReconnection:m0 = 0.3");
    pythia.readString("ColourReconnection:allowJunctions = on");
    pythia.readString("ColourReconnection:junctionCorrection = 1.2");
    pythia.readString("ColourReconnection:timeDilationMode = 2");
    pythia.readString("ColourReconnection:timeDilationPar = 0.18");
    if(!kRopes)
pythia.readString("Ropewalk:RopeHadronization = off");
  }


pythia.readString("ParticleDecays:limitTau0=on");
pythia.readString("ParticleDecays:tauMax=10");

pythia.readString("Random:setSeed = on");
pythia.readString(Form("Random:seed = %i",nfile+1));
```